Available online at www.sciencedirect.com
SCIENCE DIRECT®
International Journal of Solids and Structures 43 (2006) 1159–1188
INTERNATIONAL JOURNAL OF SOLIDS and STRUCTURES
www.elsevier.com/locate/ijsolstr

Energy release rate and contact zone in a cohesive and an interface crack by hypersingular integral equations

B. Kilic [a], E. Madenci [a,*], R. Mahajan [b]

[a] *Department of Aerospace and Mechanical Engineering, The University of Arizona, Tucson, AZ 85721, USA*
[b] *Assembly Technology Development, Intel Corporation, Chandler, AZ 85226, USA*

Received 3 November 2004; received in revised form 31 May 2005
Available online 20 July 2005

Abstract

Solution of Cauchy-type singular integral equations permits the evaluation of the fracture parameters at the crack tips very accurately. However, it does not permit the determination of the crack opening and sliding displacements while ensuring no crack surface interpenetration unless the location of the contact zone is known a priori. In order to circumvent this shortcoming, this study presents a solution method based on the Hadamard-type singular integral equations to obtain the crack opening and sliding displacements directly while enforcing the appropriate conditions to prevent interpenetration. Furthermore, the crack opening displacements are physically more meaningful and readily validated against the finite element analysis predictions. The numerical solutions of the hypersingular integral equations provide not only crack opening and sliding displacements directly but also the stress intensity factors and energy release rates. Also, the behavior of the energy release rate is examined as the cohesive crack located parallel to the interface approaches the interface from either the soft or the stiff side of the interface. The limiting value of the energy release rate is established by considering an interface crack. As the cohesive crack approaches the interface from either side of the interface, the energy release rate approaches to that of the interface crack. However, the length of contact zone between the cohesive crack surfaces under uniform shear loading does not approach to that of the interface crack.

Keywords: Interface crack; Energy release rate; Hadamard-type singularity

* Corresponding author. Tel.: +1 520 621 6113; fax: +1 520 621 8191.
E-mail address: madenci@email.arizona.edu (E. Madenci).

0020-7683/$ - see front matter © 2005 Elsevier Ltd. All rights reserved.
doi:10.1016/j.ijsolstr.2005.06.005

1. Introduction

In the construction of aircraft and space structures or electronic devices, the fusion process and adhesion are the primary means for joining different materials. However, the interface between dissimilar materials is always prone to imperfections. If the bond is not sufficiently strong, it delaminates along the interface. If the bond is too strong to delaminate, the cracking (cohesive failure) occurs in the weakest of the adjoining materials. Within the realm of linear elasticity theory, the stress states associated with a cohesive crack embedded in a homogeneous medium and an interface crack are different in nature. Therefore, the initial location of the crack tip plays a vital role in the analysis of dissimilar materials having a crack. If the cracking is of cohesive type as shown in Fig. 1, the well-established square root singularity prevails at the crack tips. However, the presence of a crack along the interface induces an oscillating stress singularity with a very rapid reversal of sign as the tip of the crack is approached according to Williams (1959). As pointed out by England (1965), Erdogan (1965), Rice and Sih (1965) and Malyshev and Salganik (1965), this peculiar oscillatory singularity leads to the wrinkling of the crack faces and overlapping (interpenetration) of the material. England showed that this kind of oscillatory singularity is physically inadmissible but is confined to a very small region near the crack tips. Erdogan (1965) suggested that this interpenetration is not significant in practical terms because it is confined to a very small region. This situation is analogous to the homogeneous case wherein the unbounded stresses are physically impossible and mathematically anomalous. However, they provide useful information when the extent of their singular behavior is contained within a small region.

To correct the physical inadmissibility of crack surface interpenetration, Comninou (1977) addressed the apparent physical inconsistency of the oscillatory stress field by using a model that imposed contact zones ahead of the crack tips. Subjected to a tensile loading, the contact zone near the crack tip is found to be on the order of 10^{-4} and that the oscillatory character of the stress field disappears. Also, only the shear stress is singular ahead of the crack tip, while the normal stress is tensile but finite. However, the global nature of the stress field is very close to that of a fully opened crack which possesses an oscillatory singularity. Therefore, the oscillatory characteristic can be considered an artifact of the linear elastic analysis and confined to a region extremely close to the crack tip. Atkinson (1977, 1982) concluded that the solutions with an oscillatory stress field are valid only away from the crack tip in the sense of asymptotic expansions. Thus, the solutions using the oscillatory character adequately model the near and far field stresses outside the region of interpenetration.

While the crack surface interpenetration can be removed by imposing contact zones ahead of the crack tips, the singular stress field becomes purely anti-symmetric about the interface crack and consequently crack propagation is restricted only to the sliding mode. Although it is reasonable to expect sliding mode

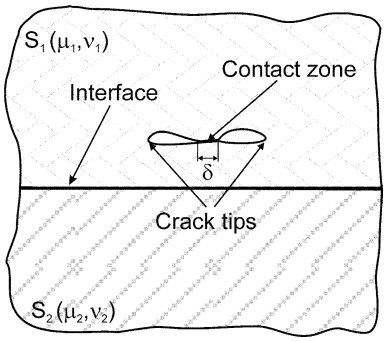

Fig. 1. Schematic for the cohesive crack with contact zone.

dominance when the material moduli differ significantly, it is unlikely that crack propagation under tension loading abruptly changes from opening mode in the case of a cohesive crack located parallel to an interface to a pure sliding mode in the case of an interface crack upon the introduction of a simple discontinuity in moduli.

Subjected to combined tension and shear loading, Comninou and Schmueser (1979) and Simonov (1990) found that the extent of contact zone varies at the crack tips. At one end, the region of contact zone is always small; however, the region of contact zone at the other end may be large depending on material properties and the ratio of applied normal stress to shear stress. When the applied loading is dominated by the shear stress, the contact zone becomes significant. In the extreme case of pure shear loading, the contact zone may be as large as half of the crack length.

In determining the stress intensity factors for an interface crack with an oscillatory behavior, the previous analyses assume that the crack surfaces fully open without any contact between the opposing faces. Although this type of analysis is wrong at the scale of the contact zone, it provides acceptable stress intensity factors to characterize the near tip stress state as long as the contact zone is much smaller than crack length. If the contact zone is substantial, then this type of analysis becomes invalid.

There have been many discussions on its unusual local characteristics of an interface crack throughout the years. Its validity in a variety of situations has been clarified by Rice (1988). The singular stress field directly ahead of the crack tip is characterized by the complex stress intensity factor whose real and imaginary parts no longer represent the usual definitions of the stress intensity factors for the opening and shearing modes of a crack in a homogeneous material. There have been varying definitions of the stress intensity factor for the purpose of characterizing the near tip field of an interfacial crack. Most of these definitions differ from one another only by a phase factor (Rice and Sih, 1965; Erdogan, 1965; Rice, 1988). The interface crack induces both opening and shearing mode behavior even under single mode of loading. The tensile and shear effects near the crack tips are intrinsically inseparable.

A more in depth treatment of interfacial fracture mechanics for isotropic materials is given by Rice (1988) and Suo and Hutchinson (1990) among others can be found in the review article by Hutchinson and Suo (1992). By introducing a characteristic length parameter, Rice (1988) eliminated the dependency of the complex stress intensity factor on the measuring unit of the crack length. However, the choice of the length parameter still remains ambiguous.

In order to remove the ambiguities associated with the characterization of an interface crack, Malyshev and Salganik (1965) considered the behavior of the total strain energy release rate in terms of the complex stress intensity factor. The strain energy release rate is well behaved even though the stress and displacement fields possess the oscillatory behavior. As observed by Mulville et al. (1976), the strain energy release rate remains relatively constant as the crack propagates along the interface.

In the previous analyses, the interface was idealized as a perfect bond line of zero thickness; however, the oscillatory singular behavior would not arise in practice because the crack tip cannot be part of two different materials at the same time. An alternative to an interface crack is the examination of a cohesive crack, free of oscillations and interpenetration, as it approaches the interface. Erdogan (1971) considered a bonded dissimilar material containing a crack parallel to the interface under the assumption that the crack surfaces fully open without any contact between the opposing crack faces. Although this model removes the interpenetration due to the oscillatory behavior of stress and displacement fields arising from material mismatch, it still leads to unacceptable interpenetration when the applied loading is dominated by the shear stress (Comninou, 1977; Erdogan and Wu, 1993). Atkinson (1977) also removed the interpenetration by introducing an intervening material between the two dissimilar materials comprising the original interface. Erdogan (1997) also discusses the mechanics and modeling issues concerning the interface cracks, and presents an extensive review.

Although the limiting value of the energy release rate can be investigated as the cohesive crack of non-oscillating character approaches the interface, there is no smooth solution method yielding transition from

one to the other. The solution method utilizing integral transformation techniques leads to a system of singular integral equations of the first kind for the cohesive crack. On the other hand, as the cohesive crack approaches the interface, the system of singular integral equations becomes one of the second kinds. In deriving the singular integral equations under the assumption that the crack fully opens, while imposing the continuity conditions along the interface and the prescribed tractions on the crack surfaces, the derivatives of the crack surface displacements serve as primary unknowns leading to Cauchy-type singular integral equations. Solution of these singular integral equations can be achieved by techniques developed by Erdogan (1969) and Erdogan and Gupta (1972) yielding the stress intensity factors. However, these solutions suffer from the interpenetration of opposing crack surfaces under the applied shear loading. Because of the nature of the primary unknowns in the singular integral equations, all of the previous studies concerning interface or cohesive cracks considered the calculation of the stress intensity factors or the energy release rate rather than the crack surface displacements.

In order to eliminate the interpenetration of the opposing crack surfaces, this study considers the crack surface displacements as primary unknowns in the derivation of the singular integral equations leading to Hadamard-type singularity. Thus, the present approach is capable of enforcing the appropriate conditions to prevent interpenetration of crack surfaces arising from the applied tractions. The crack surface displacements are physically more meaningful and easy to compare with finite element solutions which fail to provide accurate stress intensity and energy release rate without resorting to a refined mesh or a special crack-tip element.

Knowing the crack surface displacements, the energy release rate can be calculated based on the Griffith criterion that involves work done per unit depth by the applied load acting through the crack surface displacements. However, this method of calculation intrinsically assumes that the crack extension is self-similar which is erroneous in the presence of both the opening and sliding modes. Therefore, the total energy release rate defined by Malyshev and Salganik (1965) including the presence of both opening and sliding modes is computed based on the concept of crack closure introduced by Irwin (1957). Majority of the previous crack configurations concern symmetric tensile loading resulting in a gap between the crack faces. However, an interpenetration develops between the crack faces under anti-symmetric loading without the imposition of appropriate constraints at the crack faces. Regardless of the nature of the applied loads, the interface cracks can never be fully open.

Similar to the investigation by Erdogan and Joseph (1988), this study examines the behavior of the energy release rate as the cohesive crack located parallel to the interface approaches the interface from either side, and its limiting value is established by considering an interface crack. Unlike the previous study by Erdogan and Joseph (1988), the present study imposes the appropriate constraints to prevent interpenetration of the crack surfaces by considering the crack surface displacements as primary unknowns in the derivation of the singular integral equations. The description of the geometry and the crack configurations are shown in the next section. The solution method and the numerical analysis of the singular integral equations with Hadamard-type singularity are described in the subsequent sections. The numerical results concern the energy release rate calculations and the crack surface displacements.

2. Problem statement

As shown in Fig. 2, a crack located parallel to the interface of dissimilar materials is considered under symmetric and anti-symmetric tractions acting on the crack surfaces while preventing crack surface interpenetration. This crack configuration was previously investigated by Erdogan (1971) under the assumption of a fully open crack for both type of loading conditions leading to singular integral equations with Cauchy-type singularity. As a special case of this configuration, an interface crack shown in Fig. 3 is also considered to establish the limiting values of the strain energy release rate as the cohesive (homogeneous) crack approaches the interface.

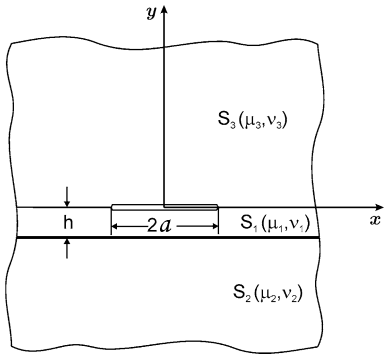

Fig. 2. Crack geometry and notation for a cohesive crack.

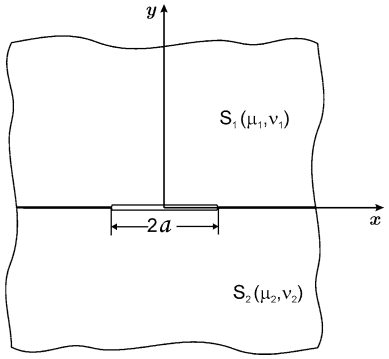

Fig. 3. Crack geometry and notation for an interface crack.

The crack configuration with respect to the interface of two dissimilar materials is described in Fig. 2. The crack with a length of $2a$, situated at a distance h from the interface lies along the x-axis of the Cartesian coordinate system (x, y) whose origin is located at the crack center. The other length parameters are normalized with respect to half of the crack length which is taken to be unity, i.e., $a = 1$, without any loss of generality. The geometry possesses symmetry with respect to $x = 0$ plane. As shown in Fig. 2, the material on the upper part of the interface is divided into two regions denoted by S_1 and S_3. The material between the planes of crack and interface is represented by region, S_1. The material on the upper part of the crack is in region, S_3. The material on the lower part of the interface occupies the region denoted by S_2. The material in each region is isotropic, elastic, and homogeneous, with shear moduli, $\mu_1 = \mu_3$, μ_2 and Poisson's ratios, $\nu_1 = \nu_3$, ν_2.

The displacement equilibrium equations in each region are

$$\mu_i \nabla^2 u_i + (\lambda_i + \mu_i) \frac{\partial}{\partial x}\left(\frac{\partial u_i}{\partial x} + \frac{\partial v_i}{\partial y}\right) = 0 \tag{1a}$$

$$\mu_i \nabla^2 v_i + (\lambda_i + \mu_i) \frac{\partial}{\partial y}\left(\frac{\partial u_i}{\partial x} + \frac{\partial v_i}{\partial y}\right) = 0 \tag{1b}$$

where u_i and v_i are the components of the displacement field along the x and y directions, and λ_i is Lame's constant with $(i = 1, 2, 3)$. The subscripted (or superscripted) i refers to the regions. Using the stress–strain and kinematic relations, the stress components can be expressed as

$$\sigma_{xx}^{(i)} = \frac{\mu_i}{\kappa_i - 1}\left[(1+\kappa_i)\frac{\partial u_i}{\partial x} + (3-\kappa_i)\frac{\partial v_i}{\partial y}\right] \tag{2a}$$

$$\sigma_{yy}^{(i)} = \frac{\mu_i}{\kappa_i - 1}\left[(1+\kappa_i)\frac{\partial v_i}{\partial y} + (3-\kappa_i)\frac{\partial u_i}{\partial x}\right] \tag{2b}$$

and

$$\sigma_{xy}^{(i)} = \mu_i\left(\frac{\partial u_i}{\partial y} + \frac{\partial v_i}{\partial x}\right) \tag{2c}$$

in which $\kappa_i = 3 - 4\nu_i$ and $\kappa_i = \frac{3-\nu_i}{1+\nu_i}$ for plane strain and stress conditions, respectively.

Along the interface plane of $y = -h$ between regions of S_1 and S_2, the continuity of displacement and traction components requires that

$$u_1(x,-h) = u_2(x,-h) \quad 0 < |x| < \infty \tag{3a}$$

$$v_1(x,-h) = v_2(x,-h) \quad 0 < |x| < \infty \tag{3b}$$

$$\sigma_{yy}^{(1)}(x,-h) = \sigma_{yy}^{(2)}(x,-h) \quad 0 < |x| < \infty \tag{3c}$$

$$\sigma_{xy}^{(1)}(x,-h) = \sigma_{xy}^{(2)}(x,-h) \quad 0 < |x| < \infty \tag{3d}$$

The applied tractions on the upper and lower crack surfaces of $y = 0^+$ and $y = 0^-$ planes, respectively, are specified as

$$\lim_{y\to 0^-} \sigma_{yy}^{(1)}(x,y) = \lim_{y\to 0^+} \sigma_{yy}^{(3)}(x,y) = p(x) \quad 0 < |x| < a \tag{4a}$$

$$\lim_{y\to 0^-} \sigma_{xy}^{(1)}(x,y) = \lim_{y\to 0^+} \sigma_{xy}^{(3)}(x,y) = q(x) \quad 0 < |x| < a \tag{4b}$$

in which the applied normal, $p(x)$ and shear, $q(x)$ tractions have the properties of

$$p(x) = (-1)^{\ell} p(-x) \quad \text{and} \quad q(x) = (-1)^{\ell+1} q(-x) \tag{5}$$

where the parameter, $\ell = 0$ and $\ell = 1$ denotes the symmetric and anti-symmetric tractions on the crack surfaces, respectively. The continuity of displacement and traction components along the crack plane of $y = 0$ requires that

$$\lim_{y\to 0^-} u_1(x,y) = \lim_{y\to 0^+} u_3(x,y) \quad a \leqslant |x| < \infty \tag{6a}$$

$$\lim_{y\to 0^-} v_1(x,y) = \lim_{y\to 0^+} v_3(x,y) \quad a \leqslant |x| < \infty \tag{6b}$$

$$\lim_{y\to 0^-} \sigma_{yy}^{(1)}(x,y) = \lim_{y\to 0^+} \sigma_{yy}^{(3)}(x,y) \quad a < |x| < \infty \tag{6c}$$

$$\lim_{y\to 0^-} \sigma_{xy}^{(1)}(x,y) = \lim_{y\to 0^+} \sigma_{xy}^{(3)}(x,y) \quad a < |x| < \infty \tag{6d}$$

The interpenetration of the crack surfaces is prevented by introducing a contact zone along which crack opening is not permitted by imposing the condition of

$$v_1(x,0^+) = v_3(x,0^-) \quad c_0 \leqslant x \leqslant c_1 \tag{7}$$

in which c_0 is the unknown distance from the center of crack where the contact zone starts, and c_1 is the unknown distance from the center of crack where the contact zone ends. Therefore, $\delta = c_1 - c_0$ specifies the extent of the contact zone as shown in Fig. 1. Finally, the far field regularity conditions require that

$$u_i, v_i \to 0 \quad \text{for } x \to \infty \text{ and } y \to \infty \tag{8}$$

The mathematical boundary value problem then reduces to the determination of the non-trivial stress field induced by the applied tractions on the crack surfaces. The solution to this problem provides the crack opening and sliding displacements as well as the stress intensity factors and the energy release rates at the crack tips. As a special configuration, an interface crack is also considered to establish the limiting values for the energy release rate as the cohesive crack approaches the interface. Because the general loading can be expressed in terms of the combination of symmetric and anti-symmetric loads, the crack surfaces are subjected to either symmetric or anti-symmetric loads.

3. Solution procedure

The solution procedure involves the use of integral transformation techniques appropriate for mixed boundary value problems. The displacement components in each region are represented by

$$u_i(x,y) = \frac{2}{\pi}\int_0^\infty \phi_i(\alpha,y)\frac{\mathrm{d}^\ell}{\mathrm{d}(\alpha x)^\ell}(\sin(\alpha x))\mathrm{d}\alpha \tag{9a}$$

$$v_i(x,y) = \frac{2}{\pi}\int_0^\infty \psi_i(\alpha,y)(-1)^\ell\frac{\mathrm{d}^\ell}{\mathrm{d}(\alpha x)^\ell}(\cos(\alpha x))\mathrm{d}\alpha \quad (i=1,2,3) \tag{9b}$$

where $\phi_i(\alpha, y)$ and $\psi_i(\alpha, y)$ $(i = 1, 2, 3)$ are the unknown auxiliary functions, and $\ell = 0$ and $\ell = 1$ correspond to symmetric and anti-symmetric tractions on the crack surfaces, respectively.

Substitution from these integral representations into the displacement equilibrium equations, Eq. (1) leads to a pair of second order, ordinary differential equations in each region as

$$\mu_i\frac{\partial^2\phi_i}{\partial y^2} - (\lambda_i+2\mu_i)\alpha_2\phi_i - (-1)^\ell\alpha(\lambda_i+\mu_i)\frac{\partial\psi_i}{\partial y} = 0 \tag{10a}$$

$$(-1)^\ell\alpha(\lambda_i+\mu_i)\frac{\partial\phi_i}{\partial y} + (\lambda_i+2\mu_i)\frac{\partial^2\psi_i}{\partial y^2} - \mu_i\alpha_2\psi_i = 0 \tag{10b}$$

The general solution to these systems of equations can be readily written as

$$\begin{Bmatrix}\phi_i\\ \psi_i\end{Bmatrix} = \left[A_{i1}\begin{Bmatrix}1\\ (-1)^\ell\end{Bmatrix} + A_{i2}\left(\begin{Bmatrix}1\\ (-1)^\ell\end{Bmatrix}y + \begin{Bmatrix}0\\ \kappa_i/\alpha(-1)^\ell\end{Bmatrix}\right)\right]\mathrm{e}^{-\alpha y} + \left[A_{i3}\begin{Bmatrix}1\\ (-1)^{\ell+1}\end{Bmatrix} + A_{i4}\left(\begin{Bmatrix}1\\ (-1)^{\ell+1}\end{Bmatrix}y + \begin{Bmatrix}0\\ \kappa_i/\alpha(-1)^\ell\end{Bmatrix}\right)\right]\mathrm{e}^{\alpha y} \tag{11}$$

where $A_{ij}(\alpha)$ $(i = 1, 2, 3$ and $j = 1, 2, 3, 4)$ are the unknown coefficients to be determined from the boundary and continuity conditions.

Invoking the far field regularity conditions, Eq. (8) permits the determination of

$$A_{33} = A_{34} = A_{21} = A_{22} = 0 \tag{12}$$

Enforcing the continuity of tractions, Eqs. (6c) and (6d) along the crack plane of $y = 0$ between regions S_1 and S_3, and the continuity conditions, Eq. (3) along the interface plane of $y = -h$ between regions S_1 and S_2 permits the determination of A_{11}, A_{12}, A_{23}, A_{24}, A_{31} and A_{32} in terms of A_{13} and A_{14}. The explicit expressions for these coefficients that are identical for both symmetric and anti-symmetric tractions on the crack surfaces are given in Appendix A.

Substituting for these coefficients in the expressions for the continuity of displacement components, Eqs. (5a) and (5b) along the crack plane of $y = 0$ leads to

$$u_3(x,0^+)-u_1(x,0^-)=-(1+\kappa_1)\frac{2}{\pi}\int_0^\infty\left(A_{13}+\frac{(1-\kappa_1)}{2\alpha}A_{14}\right)\frac{\mathrm{d}^\ell}{\mathrm{d}(\alpha x)^\ell}(\sin(\alpha x))\mathrm{d}\alpha=0\quad(y=0,|x|\geqslant a) \tag{13a}$$

$$v_3(x,0^+)-v_1(x,0^-)=(1+\kappa_1)\frac{2}{\pi}\int_0^\infty\left(A_{13}-\frac{(1+\kappa_1)}{2\alpha}A_{14}\right)\frac{\mathrm{d}^\ell}{\mathrm{d}(\alpha x)^\ell}(\cos(\alpha x))\mathrm{d}\alpha=0\quad(y=0,|x|\geqslant a) \tag{13b}$$

Imposing the applied tractions, Eq. (4) on the crack surfaces leads to

$$\lim_{y\to0^-}\sigma_{yy}^{(1)}(x,y)=\lim_{y\to0^-}\int_0^\infty\hat{\sigma}_{yy}^{(1)}(\alpha,y)\frac{\mathrm{d}^\ell}{\mathrm{d}(\alpha x)^\ell}(\cos(\alpha x))\mathrm{d}\alpha=\frac{\pi}{2}p(x)\quad(y=0,|x|<a) \tag{14a}$$

$$\lim_{y\to0^-}\sigma_{xy}^{(1)}(x,y)=\lim_{y\to0^-}\int_0^\infty\hat{\sigma}_{xy}^{(1)}(\alpha,y)\frac{\mathrm{d}^\ell}{\mathrm{d}(\alpha x)^\ell}(\sin(\alpha x))\mathrm{d}\alpha=\frac{\pi}{2}q(x)\quad(y=0,|x|<a) \tag{14b}$$

where

$$\begin{aligned}\hat{\sigma}_{yy}^{(1)}(\alpha,y)&=2\alpha\mu_1(a_1(1+2\alpha(h+y))\mathrm{e}^{-\alpha(2h+y)}-\mathrm{e}^{\alpha y})A_{13}+\mu_1(1+\kappa_1-2\alpha y)\mathrm{e}^{\alpha y}A_{14}\\&+\mu_1((1+\kappa_1)\mu_1(\kappa_1/(\kappa_1\mu_2+\mu_1)-\kappa_2/(\kappa_2\mu_1+\mu_2))-4\alpha^2h^2a_1)\mathrm{e}^{-\alpha(2h+y)}A_{14}\\&-\mu_1a_1(2\alpha h+\kappa_1)(1+\kappa_1+2\alpha y)\mathrm{e}^{-\alpha(2h+y)}A_{14}\end{aligned} \tag{15a}$$

and

$$\begin{aligned}\hat{\sigma}_{xy}^{(1)}(\alpha,y)&=2\alpha\mu_1(a_1(-1+2\alpha(h+y))\mathrm{e}^{-\alpha(2h+y)}+\mathrm{e}^{\alpha y})A_{13}+\mu_1(1-\kappa_1+2\alpha y)\mathrm{e}^{\alpha y}A_{14}\\&+\mu_1((1+\kappa_1)\mu_1(\kappa_1/(\kappa_1\mu_2+\mu_1)-\kappa_2/(\kappa_2\mu_1+\mu_2))-4\alpha^2h^2a_1)\mathrm{e}^{-\alpha(2h+y)}A_{14}\\&-\mu_1a_1(2\alpha h+\kappa_1)(-1+\kappa_1+2\alpha y)\mathrm{e}^{-\alpha(2h+y)}A_{14}\end{aligned} \tag{15b}$$

in which the constant a_1 is defined as $a_1=\frac{\mu_1-\mu_2}{\mu_1+\kappa_1\mu_2}$.

Representing the opening and sliding of the crack surfaces by the unknown auxiliary functions $U(x)$ and $V(x)$ in the form

$$u_3(x,0^+)-u_1(x,0^-)=U(x)H(a-x) \tag{16a}$$

$$v_3(x,0^+)-v_1(x,0^-)=V(x)H(a-x) \tag{16b}$$

ensures the continuity of the displacement components, Eqs. (5a) and (5b) along the crack plane. The Heaviside step function is represented by $H(x)$. Note that these unknown functions, $U(x)$ and $V(x)$ have the property of

$$U(x)=(-1)^{\ell+1}U(-x)\quad\text{and}\quad V(x)=(-1)^\ell V(-x) \tag{17}$$

Invoking these unknown functions into Eq. (13) and solving for A_{13} and A_{14} result in

$$A_{13}=-\frac{1}{2(1+\kappa_1)}\int_0^\infty\left((1+\kappa_1)U(x)\frac{\mathrm{d}^\ell}{\mathrm{d}(\alpha x)^\ell}(\sin(\alpha x))-(1-\kappa_1)V(x)\frac{\mathrm{d}^\ell}{\mathrm{d}(\alpha x)^\ell}(\cos(\alpha x))\right)\mathrm{d}x \tag{18a}$$

and

$$A_{14} = -\frac{1}{(1+\kappa_1)}\alpha\int_0^\infty \left(U(x)\frac{\mathrm{d}^\ell}{\mathrm{d}(\alpha x)^\ell}(\sin(\alpha x)) + V(x)\frac{\mathrm{d}^\ell}{\mathrm{d}(\alpha x)^\ell}(\cos(\alpha x)) \right)\mathrm{d}x \tag{18b}$$

Substituting for A_{13} and A_{14} in Eq. (14) and performing the appropriate limit operation leads to

$$\begin{aligned} &-\lim_{y\to 0^-}\int_0^1 \mathrm{d}t\, V(t)\int_0^\infty \alpha \mathrm{e}^{\alpha y}\frac{\mathrm{d}^\ell}{\mathrm{d}(\alpha t)^\ell}(\cos(\alpha t))\frac{\mathrm{d}^\ell}{\mathrm{d}(\alpha x)^\ell}(\cos(\alpha x))\mathrm{d}\alpha \\ &+\int_0^1 \mathrm{d}t\, U(t)\int_0^\infty \mathscr{A}(\alpha)\frac{\mathrm{d}^\ell}{\mathrm{d}(\alpha t)^\ell}(\sin(\alpha t))\frac{\mathrm{d}^\ell}{\mathrm{d}(\alpha x)^\ell}(\cos(\alpha x))\mathrm{d}\alpha \\ &+\int_0^1 \mathrm{d}t\, V(t)\int_0^\infty \mathscr{B}(\alpha)\frac{\mathrm{d}^\ell}{\mathrm{d}(\alpha t)^\ell}(\cos(\alpha t))\frac{\mathrm{d}^\ell}{\mathrm{d}(\alpha x)^\ell}(\cos(\alpha x))\mathrm{d}\alpha = \frac{\pi}{2}\frac{1+\kappa_1}{2\mu_1}p(x) \end{aligned} \tag{19a}$$

and

$$\begin{aligned} &-\lim_{y\to 0^-}\int_0^1 \mathrm{d}t\, U(t)\int_0^\infty \alpha \mathrm{e}^{\alpha y}\frac{\mathrm{d}^\ell}{\mathrm{d}(\alpha t)^\ell}(\sin(\alpha t))\frac{\mathrm{d}^\ell}{\mathrm{d}(\alpha x)^\ell}(\sin(\alpha x))\mathrm{d}\alpha \\ &+\int_0^1 \mathrm{d}t\, U(t)\int_0^\infty \mathscr{C}(\alpha)\frac{\mathrm{d}^\ell}{\mathrm{d}(\alpha t)^\ell}(\sin(\alpha t))\frac{\mathrm{d}^\ell}{\mathrm{d}(\alpha x)^\ell}(\sin(\alpha x))\mathrm{d}\alpha \\ &+\int_0^1 \mathrm{d}t\, V(t)\int_0^\infty \mathscr{D}(\alpha)\frac{\mathrm{d}^\ell}{\mathrm{d}(\alpha t)^\ell}(\cos(\alpha t))\frac{\mathrm{d}^\ell}{\mathrm{d}(\alpha x)^\ell}(\sin(\alpha x))\mathrm{d}\alpha = \frac{\pi}{2}\frac{1+\kappa_1}{2\mu_1}q(x) \end{aligned} \tag{19b}$$

where the coefficients $\mathscr{A}(\alpha)$, $\mathscr{B}(\alpha)$, $\mathscr{C}(\alpha)$ and $\mathscr{D}(\alpha)$ are expressed as

$$\mathscr{A}(\alpha) = \alpha(-\gamma_1 + 2a_1h^2\alpha^2)\mathrm{e}^{-2h\alpha} \tag{20a}$$

$$\mathscr{B}(\alpha) = \alpha(\gamma_2 + 2a_1h\alpha(1+h\alpha))\mathrm{e}^{-2h\alpha} \tag{20b}$$

$$\mathscr{C}(\alpha) = \alpha(\gamma_2 + 2a_1h\alpha(-1+h\alpha))\mathrm{e}^{-2h\alpha} \tag{20c}$$

$$\mathscr{D}(\alpha) = \alpha(-\gamma_1 + 2a_1h^2\alpha^2)\mathrm{e}^{-2h\alpha} \tag{20d}$$

in which the known constants are defined by

$$\gamma_1 = \left(\frac{a_1}{2} + a_2\right) \quad \text{and} \quad \gamma_2 = \left(\frac{a_1}{2} - a_2\right)$$

with

$$a_1 = \frac{\mu_1 - \mu_2}{\mu_1 + \kappa_1\mu_2} \quad \text{and} \quad a_2 = \frac{\kappa_1\mu_2 - \kappa_2\mu_1}{2(\mu_2 + \kappa_2\mu_1)}$$

Considering symmetry properties of $U(x)$ and $V(x)$ and evaluating the infinite integrals in Eq. (19) lead to a pair of integral equations with Hadamard-type singularity as

$$\frac{1}{\pi}\int_{-1}^1 \frac{V(t)}{(t-x)^2}\mathrm{d}t + \int_{-1}^1 V(t)K_{11}(x,t)\mathrm{d}t + \int_{-1}^1 U(t)K_{12}(x,t)\mathrm{d}t = \frac{1+\kappa_1}{2\mu_1}p(x) \tag{21a}$$

$$\frac{1}{\pi}\int_{-1}^1 \frac{U(t)}{(t-x)^2}\mathrm{d}t + \int_{-1}^1 V(t)K_{21}(x,t)\mathrm{d}t + \int_{-1}^1 U(t)K_{22}(x,t)\mathrm{d}t = \frac{1+\kappa_1}{2\mu_1}q(x) \tag{21b}$$

where the kernels are defined as

$$K_{11}(x,t)=\frac{1}{\pi}\left[\gamma_2\frac{4h^2-(t-x)^2}{\left((t-x)^2+4h^2\right)^2}+8a_1h^2\frac{4h^2-3(t-x)^2}{\left((t-x)^2+4h^2\right)^3}+12a_1h^2\frac{16h^4-24h^2(t-x)^2+(t-x)^4}{\left((t-x)^2+4h^2\right)^4}\right]$$

$$K_{12}(x,t)=\frac{1}{\pi}\left[-4h\gamma_1\frac{t-x}{\left((t-x)^2+4h^2\right)^2}+96a_1h^3\frac{(t-x)(4h^2-(t-x)^2)}{\left((t-x)^2+4h^2\right)^4}\right]$$

$$K_{21}(x,t)=-K_{12}(x,t)$$

$$K_{22}(x,t)=\frac{1}{\pi}\left[\gamma_2\frac{4h^2-(t-x)^2}{\left((t-x)^2+4h^2\right)^2}-8a_1h^2\frac{(4h^2-3(t-x)^2)}{\left((t-x)^2+4h^2\right)^3}+12a_1h^2\frac{16h^4-24h^2(t-x)^2+(t-x)^4}{\left((t-x)^2+4h^2\right)^4}\right]$$

By using the function-theoretic method of Muskhelishvili (1992) and the properties of hypersingular integral equations described by Ioakimidis (1988a,b, 1990), Kaya (1984), Kaya and Erdogan (1987) and later by Chan et al. (2003), the solution form of $U(x)$ and $V(x)$ in these integral equations, Eqs. (21a) and (21b), can be represented by

$$V(x)=G_1(x)\sqrt{1-x^2} \tag{22a}$$

$$U(x)=G_2(x)\sqrt{1-x^2} \tag{22b}$$

where $G_1(x)$ and $G_2(x)$ are the new unknown bounded functions.

In accordance with Irwin (1957), the singular stress field directly ahead of the crack tip is characterized by the stress intensity factors in the form

$$\sigma_{xx}+\mathrm{i}\sigma_{xy}=\lim_{r\to 0}\frac{k_1+\mathrm{i}k_2}{\sqrt{2r}} \tag{23}$$

where k_1 and k_2 represent the stress intensity factors related to the opening and sliding modes, respectively, and r is the distance from crack tip.

Utilizing Eqs. (22a) and (22b), the stress intensity factors for opening and sliding modes can be evaluated as

$$k_1(1)=\lim_{x\to 1}\sqrt{(x^2-1)}\sigma_{yy}(x)=\frac{2\mu_1}{1+\kappa_1}\lim_{x\to 1}\frac{V(x)}{\sqrt{1-x^2}}=\frac{2\mu_1}{1+\kappa_1}G_1(1) \tag{24a}$$

$$k_1(-1)=\lim_{x\to -1}\sqrt{(x^2-1)}\sigma_{yy}(x)=\frac{2\mu_1}{1+\kappa_1}\lim_{x\to -1}\frac{V(x)}{\sqrt{1-x^2}}=\frac{2\mu_1}{1+\kappa_1}G_1(-1) \tag{24b}$$

$$k_2(1)=\lim_{x\to 1}\sqrt{(x^2-1)}\sigma_{xy}(x)=\frac{2\mu_1}{1+\kappa_1}\lim_{x\to 1}\frac{U(x)}{\sqrt{1-x^2}}=\frac{2\mu_1}{1+\kappa_1}G_2(1) \tag{24c}$$

$$k_2(-1)=\lim_{x\to -1}\sqrt{(x^2-1)}\sigma_{xy}(x)=\frac{2\mu_1}{1+\kappa_1}\lim_{x\to -1}\frac{U(x)}{\sqrt{1-x^2}}=\frac{2\mu_1}{1+\kappa_1}G_2(-1) \tag{24d}$$

The total energy release rate can be written in terms of stress intensity factors as

$$\mathscr{G}=\mathscr{G}_1+\mathscr{G}_2=\frac{\pi(1+\kappa_1)}{4\mu_1}(k_1^2+k_2^2) \tag{25}$$

The explicit form of the singular integral equations for an interface crack can be derived as the distance, h approaches zero, i.e., $h\to 0^+$ in Eq. (19), resulting in

$$-\lim_{y\to 0^-}\int_0^1 \mathrm{d}t\,V(t)\int_0^\infty \alpha e^{\alpha y}\frac{\mathrm{d}^\ell}{\mathrm{d}(\alpha t)^\ell}(\cos(\alpha t))\frac{\mathrm{d}^\ell}{\mathrm{d}(\alpha x)^\ell}(\cos(\alpha x))\mathrm{d}\alpha$$
$$-\gamma_1\lim_{h\to 0^+}\int_0^1 \mathrm{d}t\,U(t)\int_0^\infty \alpha e^{-2h\alpha}\frac{\mathrm{d}^\ell}{\mathrm{d}(\alpha t)^\ell}(\sin(\alpha t))\frac{d^\ell}{\mathrm{d}(\alpha x)^\ell}(\cos(\alpha x))\mathrm{d}\alpha$$
$$+\gamma_2\lim_{h\to 0^+}\int_0^1 \mathrm{d}t\,V(t)\int_0^\infty \alpha e^{-2h\alpha}\frac{\mathrm{d}^\ell}{\mathrm{d}(\alpha t)^\ell}(\cos(\alpha t))\frac{\mathrm{d}^\ell}{\mathrm{d}(\alpha x)^\ell}(\cos(\alpha x))\mathrm{d}\alpha=\frac{\pi}{2}\frac{1+\kappa_1}{2\mu_1}p(x) \tag{26a}$$

and

$$-\lim_{y\to 0^-}\int_0^1 \mathrm{d}t\,U(t)\int_0^\infty \alpha e^{\alpha y}\frac{\mathrm{d}^\ell}{\mathrm{d}(\alpha t)^\ell}(\sin(\alpha t))\frac{\mathrm{d}^\ell}{\mathrm{d}(\alpha x)^\ell}(\sin(\alpha x))\mathrm{d}\alpha$$
$$+\gamma_2\lim_{h\to 0^+}\int_0^1 \mathrm{d}t\,U(t)\int_0^\infty \alpha e^{-2h\alpha}\frac{\mathrm{d}^\ell}{\mathrm{d}(\alpha t)^\ell}(\sin(\alpha t))\frac{\mathrm{d}^\ell}{\mathrm{d}(\alpha x)^\ell}(\sin(\alpha x))\mathrm{d}\alpha$$
$$-\gamma_1\lim_{h\to 0^+}\int_0^1 \mathrm{d}t\,V(t)\int_0^\infty \alpha e^{-2h\alpha}\frac{\mathrm{d}^\ell}{\mathrm{d}(\alpha t)^\ell}(\cos(\alpha t))\frac{\mathrm{d}^\ell}{\mathrm{d}(\alpha x)^\ell}(\sin(\alpha x))\mathrm{d}\alpha=\frac{\pi}{2}\frac{1+\kappa_1}{2\mu_1}q(x) \tag{26b}$$

After defining $2h=-y$ and changing the appropriate variable in these equations, and evaluating the appropriate infinite integrals, these expressions can be rewritten as

$$\frac{1}{2}(\gamma_2-1)\lim_{y\to 0^-}\int_0^1 \mathrm{d}t\,V(t)\left(\frac{y^2-(t-x)^2}{((t-x)^2+y^2)^2}+(-1)^\ell\frac{y^2-(t+x)^2}{((t+x)^2+y^2)^2}\right)$$
$$-\frac{1}{2}\gamma_1\lim_{y\to 0^-}\int_0^1 \mathrm{d}t\,U(t)\int_0^\infty \mathrm{d}\alpha\,\alpha e^{\alpha y}(\sin\alpha(t-x)+(-1)^\ell\sin\alpha(t+x))=\frac{\pi}{2}\frac{1+\kappa_1}{2\mu_1}p(x) \tag{27a}$$

and

$$\frac{1}{2}(\gamma_2-1)\lim_{y\to 0^-}\int_0^1 \mathrm{d}t\,U(t)\left(\frac{y^2-(t-x)^2}{((t-x)^2+y^2)^2}-(-1)^\ell\frac{y^2-(t+x)^2}{((t+x)^2+y^2)^2}\right)$$
$$+\frac{1}{2}\gamma_1\lim_{y\to 0^-}\int_0^1 \mathrm{d}t\,V(t)\int_0^\infty \mathrm{d}\alpha\,\alpha e^{\alpha y}(\sin\alpha(t-x)-(-1)^\ell\sin\alpha(t+x))=\frac{\pi}{2}\frac{1+\kappa_1}{2\mu_1}q(x) \tag{27b}$$

By performing the limit operation and evaluating the infinite integrals while considering symmetry properties of $U(x)$ and $V(x)$, these equations are further reduced to

$$\frac{1}{\pi}\int_{-1}^1 \mathrm{d}t\frac{V(t)}{(t-x)^2}-\gamma\frac{\mathrm{d}U}{\mathrm{d}x}(x)=\frac{1+\kappa_1}{2\mu_1(1-\gamma_2)}p(x) \tag{28a}$$

and

$$\frac{1}{\pi}\int_{-1}^1 \mathrm{d}t\frac{U(t)}{(t-x)^2}+\gamma\frac{\mathrm{d}V}{\mathrm{d}x}(x)=\frac{1+\kappa_1}{2\mu_1(1-\gamma_2)}q(x) \tag{28b}$$

where $\gamma=\frac{\gamma_1}{1-\gamma_2}$. Knowing that any function can be decomposed into the sum of even and odd functions, these integral equations are valid for general loading functions.

These integro-differential equations can be combined into the following final form by multiplying Eq. (28a) by $-\mathrm{i}$ and adding to (28b):

$$\frac{1}{\pi\mathrm{i}}\int_{-1}^1 \mathrm{d}t\frac{f(t)}{(t-x)^2}+\gamma\frac{\mathrm{d}f(x)}{\mathrm{d}x}=\frac{1}{2\mu_0}(q(x)-\mathrm{i}p(x)) \tag{29}$$

where $\mu_0 = \mu_1 \frac{1-\gamma_2}{1+\kappa_1}$ and the auxiliary function, $f(x)$ is defined as

$$f(x) = V(x) + \mathrm{i}U(x) \tag{30}$$

Analogous to the solution of Eq. (21), the solution to this integral equation, $f(x)$ can be represented by

$$f(x) = \frac{G_0(x)}{(1-x)^{\alpha}(1+x)^{\beta}} \tag{31}$$

where $G_0(x)$ is an unknown bounded function and

$$\alpha = -\frac{1}{2} + \mathrm{i}\omega, \quad \beta = -\frac{1}{2} - \mathrm{i}\omega \qquad \text{with } \omega = \frac{1}{2\pi}\ln\left(\frac{1-\gamma}{1+\gamma}\right) \tag{32}$$

According to Rice (1988), the singular stress field ahead of the crack tip is characterized by the complex stress intensity factor in the form

$$\sigma_{xx} + \mathrm{i}\sigma_{xy} = \lim_{r\to 0} \frac{k}{\sqrt{2r}} \left(\frac{r}{\ell}\right)^{\mathrm{i}\omega} \tag{33}$$

where r is the distance from crack tip, and $k = k_1 + \mathrm{i}k_2$ is the complex interface stress intensity factor. The characteristic length parameter, ℓ, eliminates the dependency of the complex stress intensity factor, $k = k_1 + \mathrm{i}k_2$ on the measuring unit of the crack length.

This definition is equivalent to that of Erdogan and Gupta (1971a,b) for $\ell = a$, and the stress intensity factors, k_1 and k_2 become

$$k_1 + \mathrm{i}k_2 = \lim_{x\to 1}(x-1)^{-\beta}(x+1)^{-\alpha}(\sigma_{yy} + \mathrm{i}\sigma_{xy}) \tag{34}$$

By using Eq. (31), these stress intensity factors can be expressed as

$$\frac{1}{2\mu_0\sqrt{1-\gamma_2}}(k_1(1) + \mathrm{i}k_2(1)) = -2\alpha \lim_{x\to 1}(1-x)^{\alpha}(1+x)^{\beta} f(x) = -2\alpha G_0(1) \tag{35a}$$

$$\frac{1}{2\mu_0\sqrt{1-\gamma_2}}(k_1(-1) + \mathrm{i}k_2(-1)) = -2\beta \lim_{x\to -1}(1-x)^{\alpha}(1+x)^{\beta} f(x) = -2\beta G_0(-1) \tag{35b}$$

As introduced by Erdogan and Gupta (1971a,b), the energy release rate can be related to the stress intensity factors in the form

$$\mathscr{G} = \frac{\pi}{2} \frac{(\mu_1 + \kappa_1\mu_2)(\mu_2 + \kappa_2\mu_1)}{\mu_1\mu_2[(1+\kappa_1)\mu_2 + (1+\kappa_2)\mu_1]}(k_1^2 + k_2^2) \tag{36}$$

4. Numerical analysis

The complexity of the kernels in Eqs. (21) and (29) requires that the singular integral equations be solved numerically. The solution procedure involves the reduction of the integral equations with Hadamard-type singularities to a system of linear algebraic equations using the collocation technique introduced by Miller and Keer (1985) and later extended by Quan (1991) to include the generalized Cauchy kernel, and by Kabir et al. (1998) to consider logarithmic-, Cauchy-, and Hadamard-type singularities. In this technique, the quadrature interval $[-1, 1]$ is partitioned into a series of subintervals and the integration points, t_k at the ends and midpoint of each subinterval as shown in Fig. 4. The collocation points, x_j, are defined at the midpoint of two consecutive integration points.

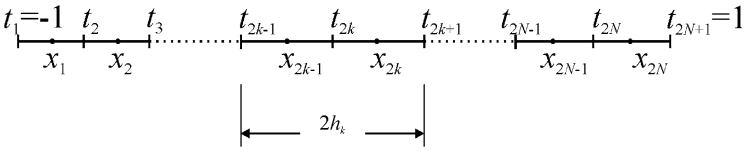

Fig. 4. Discretization of the quadrature interval.

The unknown functions, $G_i(x)$ with $i = 0, 1, 2$, defined by Eqs. (22) and (31), are approximated over each subinterval $(t_{i[2k-1]} \leqslant t \leqslant t_{i[2k+1]})$ for $k = 1, N$ by quadratic Lagrange interpolation polynomials which are given as

$$G_i(t) \approx [(t - t_{i[2k]})^2/h_{i[k]}^2 - (t - t_{i[2k]})/h_{i[k]}]G_{i[2k-1]}/2 + [1 - (t - t_{i[2k]})^2/h_{i[k]}^2]G_{i[2k]} + [(t - t_{i[2k]})^2/h_{i[k]}^2 + (t - t_{i[2k]})/h_{i[k]}]G_{i[2k+1]}/2 \tag{37}$$

where $G_{i[k]} = G_i(t_{i[k]})$ and $h_{i[k]} = (t_{i[2k+1]} - t_{i[2k-1]})/2$ with $i = 0, 1, 2$.

4.1. Cohesive crack

In the case of a cohesive crack under shear loading, in order to establish the extent of the contact zone, the normal tractions on the crack surfaces, $p(x)$ is decomposed as

$$p(x) = p_a(x) + p_r(x) \tag{38}$$

where $p_a(x)$ and $p_r(x)$ are the known applied normal tractions and unknown normal reactions, respectively. The normal reactions which cannot positive, i.e. $p_r(x) \leqslant 0$, develop if the contact zone between the crack surfaces occurs. Therefore, the normal reactions prevent the interpenetration between the opposing crack surfaces. Because the reactions are unknown, $p_r(x)$ is approximated over each subinterval $k(t_{i[k]} \leqslant t \leqslant t_{i[k+1]})$ for $k = 1, \ldots, 2N$ by linear interpolation functions given by

$$p_r(x) = \chi(x)P_{k+1} + (1 - \chi(x))P_k \tag{39}$$

in which $P_k = p_r(t_{i[k]})$ and $\chi(x) = \frac{x - t_{i[k]}}{t_{i[k+1]} - t_{i[k]}}$.

Approximation of the unknown functions, $G_1(x)$ and $G_2(x)$ and the unknown reactions on the crack surfaces, $p_r(x)$ permit the discretization of Eq. (21) as

$$\frac{1}{\pi}\sum_{i=1}^{2N_1+1} w_{1[i]}(x_j)G_{1[i]} + \sum_{i=1}^{2N_1+1} K_{11}(x_j, t_i)v_{1[i]}G_{1[i]} + \sum_{i=1}^{2N_2+1} K_{12}(x_j, t_i)v_{2[i]}G_{2[i]} = \frac{1+\kappa_1}{4\mu_1}(P_{j+1} + P_j) + \frac{1+\kappa_1}{2\mu_1}p_a(x_j) \quad j = 1, \ldots, 2N_1 \tag{40}$$

and

$$\frac{1}{\pi}\sum_{i=1}^{2N_2+1} w_{2[i]}(x_j)G_{2[i]} + \sum_{i=1}^{2N_1+1} K_{21}(x_j, t_i)v_{1[i]}G_{1[i]} + \sum_{i=1}^{2N_2+1} K_{22}(x_j, t_i)v_{2[i]}G_{2[i]} = \frac{1+\kappa_1}{2\mu_1}q(x_j) \quad j = 1, \ldots, 2N_2 \tag{41}$$

in which N_1 and N_2 are number of subintervals for unknown functions $G_1(x)$ and $G_2(x)$, respectively. The singular weight functions, $v_{i[k]}$ and $w_{i[k]}(x)$ are given by Kabir et al. (1998). Since this discretization results in a number of unknowns, $G_{i[k]}$, which are two more than the number of equations, two additional constraint equations become necessary in order to achieve a unique solution to Eqs. (40) and (41). However, the

nature of this solution method does not introduce any additional constraint equations based on the physics of the problem. As suggested by Kabir et al. (1998), the necessary additional constraint equations are obtained by multiplying the integral equations by $\sqrt{1-x^2}$ and integrating over x can be expressed in the form

$$-\int_{-1}^{1} \mathrm{d}t\, V(t) + \int_{-1}^{1} \mathrm{d}t\, V(t)\overline{K}_{11}(t) + \int_{-1}^{1} \mathrm{d}t\, V(t)\overline{K}_{12}(t) = \overline{p} \tag{42}$$

$$\int_{-1}^{1} \mathrm{d}t\, U(t) + \int_{-1}^{1} \mathrm{d}t\, V(t)\overline{K}_{21}(t) + \int_{-1}^{1} \mathrm{d}t\, V(t)\overline{K}_{22}(t) = \overline{q} \tag{43}$$

in which $\overline{K}_{ij}(t)$, $\overline{p}(x)$ and $\overline{q}(x)$ are defined as

$$\overline{K}_{ij}(t) = \int_{-1}^{1} \mathrm{d}x\, K_{ij}(x,t)\sqrt{1-x^2} \quad i,j = 1,2 \tag{44}$$

$$\overline{p} = \frac{1+\kappa_1}{2\mu_1} \int_{-1}^{1} (p_a(x) + p_r(x))\sqrt{1-x^2}\,\mathrm{d}x \tag{45}$$

$$\overline{q} = \frac{1+\kappa_1}{2\mu_1} \int_{-1}^{1} \mathrm{d}x\, q(x)\sqrt{1-x^2} \tag{46}$$

These additional constraint equations (42) and (43) are also discretized as

$$-\sum_{i=1}^{2N_1+1} v_{1[i]} G_{1[i]} + \sum_{n=1}^{2} \sum_{i=1}^{2N_n+1} \overline{K}_{1n}(t_i) v_{n[i]} G_{n[i]} = \sum_{i=1}^{2N_1} b_i^{[l]} P_i + b_i^{[r]} P_{i+1} + \overline{p}_a \tag{47}$$

and

$$-\sum_{i=1}^{2N_2+1} v_{2[i]} G_{2[i]} + \sum_{n=1}^{2} \sum_{i=1}^{2N_n+1} \overline{K}_{2n}(t_i) v_{n[i]} G_{n[i]} = \overline{q} \tag{48}$$

where $p_r(x)$ is approximated in the same manner as before, Eq. (39), and $b_i^{[l]}, b_i^{[r]}$ and $\overline{p}_a$ are defined by

$$b_i^{[l]} = \frac{1+\kappa_1}{2\mu_1} \int_{x_i}^{x_{i+1}} \mathrm{d}x\, \chi(x)\sqrt{1-x^2} \tag{49}$$

$$b_i^{[r]} = \frac{1+\kappa_1}{2\mu_1} \int_{x_i}^{x_{i+1}} \mathrm{d}x\, (1-\chi(x))\sqrt{1-x^2} \tag{50}$$

$$\overline{p}_a = \frac{1+\kappa_1}{2\mu_1} \int_{-1}^{1} \mathrm{d}x\, p_a(x)\sqrt{1-x^2} \tag{51}$$

in which $b_i^{[l]}$ and $b_i^{[r]}$ can be evaluated exactly.

The discrete form of the singular integral equations and constraint equations can be cast into the form

$$A_{ji} G_i - B_{ji} P_i = g_i \quad i,j = 1,\ldots,N \tag{52}$$

in which N is equal to $2(N_1 + N_2 + 1)$. The unknown vectors can be written as

$$\mathbf{G}^{\mathrm{T}} = \{G_{1[1]}, \ldots, G_{1[2N_1+1]}, G_{2[1]}, \ldots, G_{2[2N_2+1]}\}$$

and

$$\mathbf{P}^{\mathrm{T}} = \{P_1, \ldots, P_{2N_1+1}, 0, \ldots, 0\}$$

In the solution of Eq. (52), the unknown vectors have to satisfy the constraint equation arising from the presence of contact zones. This constraint equation can be expressed as

$$V_i = V(t_i) = 0 \quad \text{if } P_i = p_r(t_i) < 0 \tag{53a}$$

and

$$P_i = p_r(t_i) = 0 \quad \text{if } V_i = V(t_i) \geqslant 0 \tag{53b}$$

This constraint equation ensures that there is no interpenetration by enforcing the opening displacements to be equal to zero due to the presence of compressive normal reactions along the contact zone. The tensile reactions are enforced to be zero for positive crack opening displacement. As a result of this constraint equation, either the crack opening displacement, $V(t_i)$, or the reaction, $p_r(t_i)$, is equal to zero at every integration point i depending on its value. Therefore, the solution to Eq. (52) requires an iterative scheme. The solution procedure starts with assuming either $P_i = 0$ or $V_i = 0$ at every integration point.

With the assumed values of P_i or V_i, Eq. (52) having equal number of equations and unknowns can be solved directly. This linear system of equations is solved continuously by updating the status of every integration point after each solution until convergence is achieved. The status at each integration point is updated by checking Eq. (53) in which, if the constraint condition is not satisfied, the status of that point is updated for the next step by interchanging the value of $P_i = 0$ with $V_i = 0$ if P_i is positive and $V_i = 0$ with $P_i = 0$ if V_i is negative.

4.2. Interface crack

In the case of an interface crack, the approximation of the unknown function $G_0(x)$ in Eq. (31) allows discretization of Eq. (29) as

$$\frac{1}{\pi \mathrm{i}} \sum_{i=1}^{2N_0+1} w_{0[i]}(x_j) G_{0[i]} + \frac{\gamma}{(1-x_j)^{\alpha}(1+x_j)^{\beta}} \sum_{m=1}^{M} D_m h_j G_{0[L+m]} + \gamma \frac{\alpha - \beta + (\alpha+\beta)x_j}{(1-x_j)^{1+\alpha}(1+x_j)^{1+\beta}} \sum_{m=1}^{M} B_m G_{0[l+m]} = \frac{P_{j+1} + P_j}{4\mu_0 \mathrm{i}} + \frac{1}{2\mu_0}(q(x_j) - \mathrm{i}p_a(x_j)) \tag{54}$$

where I and B_m are given by Kabir et al. (1998) and h_j, L and D_m are defined in Appendix A. Similar to the discretization of equations for a cohesive crack, this discretization also results in a number of unknowns, $G_{0[k]}$ which are one more than the number of equations. Therefore, the necessary additional constraint equation is introduced by multiplying the integro-differential equation by $(1-x^2)^{3/2}$ and integrating over x, and after performing the appropriate algebraic manipulations leads to

$$\int_{-1}^{1} \mathrm{d}t \tilde{H}(t) f(t) = \tilde{g} \tag{55}$$

where $\tilde{H}(t) = 3\gamma t\sqrt{1-t^2} + \mathrm{i}3(1/2 - t^2)$ and $\tilde{g} = \frac{1}{2\mu_0}\int_{-1}^{1} \mathrm{d}x\,(q(x) - \mathrm{i}p(x))(1-x^2)^{3/2}$.

This additional constraint equation is also discretized as

$$\sum_{i=1}^{2N_0+1} \tilde{H}(t_i) v_{0[i]} G_{0[i]} = \tilde{g} \tag{56}$$

in which $\tilde{g}$ is defined by

$$\tilde{g} = \frac{1}{2\mu_0} \int_{-1}^{1} \mathrm{d}x\,(q(x) - \mathrm{i}p_a(x))(1-x^2)^{3/2} \tag{57}$$

The discrete form of the singular integral equation and constraint equation can be cast into the form

$$A_{ji}G_i = g_i \quad i,j = 1,\ldots,N \tag{58}$$

where N is equal to $2N_0 + 1$ and the unknown vector is in the form of

$$\mathbf{G}^{\mathrm{T}} = \{G_{0[1]},\ldots,G_{0[2N_0+1]}\} \tag{59}$$

In the presence of shear loading, the direct application of the approach to determine the compressive normal reactions over the contact zone and the extent of the contact zone simultaneously results in extreme numerical oscillations in the crack opening displacement. However, the solutions to both the normal reaction and the opening displacement lead to acceptable results in an average sense indicating that the oscillations in the solution is primarily due the oscillatory behavior of the unknown function. This is further validated by the fact that the frequency and magnitude of the oscillations amplify with increasing number of subintervals.

In order to alleviate and possibly eliminate this extreme oscillation in numerical results, the solution method utilizes a Cauchy-type singular integral equation obtained by integration by parts of Eq. (29). The singular integral equations with both Hadamard- and Cauchy-type singularities are then solved consecutively in an iterative manner to determine the normal reactions over the contact zone and the extent of the contact zone. By using the conditions $f(-1) = f(1) = 0$, the Cauchy-type singular integral equation is obtained as

$$\frac{1}{\pi \mathrm{i}}\int_{-1}^{1}\frac{\vartheta(t)}{t-x}\mathrm{d}t + \gamma\vartheta(x) = \frac{1}{2\mu_0}(q(x) - \mathrm{i}p(x)) \tag{60}$$

in which $\vartheta(x) = \frac{\mathrm{d}f(x)}{\mathrm{d}x} = \frac{\mathrm{d}V(x)}{\mathrm{d}x} + \mathrm{i}\frac{\mathrm{d}U(x)}{\mathrm{d}x}$.

Utilizing the function-theoretic method of Muskhelishvili (1992), the solution form of $\vartheta(x)$ can be represented by

$$\vartheta(x) = \frac{\phi(x)}{(1-x)^{-\beta}(1+x)^{-\alpha}} \tag{61}$$

where $\phi(x)$ is an unknown bounded function and α and β are defined as in Eq. (32). The solution to Eq. (60) contains one arbitrary constant which is determined by imposing the condition of single-valuedness of displacements as

$$\int_{-1}^{1}\vartheta(t)\,\mathrm{d}t = 0 \tag{62}$$

Although the exact solutions to singular integral equations with Cauchy-type singularity exist for certain simple forms of $p(x)$ and $q(x)$, the unknown normal tractions requires that the Cauchy-type singular integral equation be solved numerically subjected to the appropriate contact zone conditions. As described in the solution of Hadamard-type singular integral equations, the unknown function $\phi(x)$ is approximated over each of the subinterval by using quadratic Lagrange interpolation polynomial as given in Eq. (39). With the discretized form of the unknown function $\phi(x)$, Eqs. (60) and (62) can be rewritten as

$$\frac{1}{\pi \mathrm{i}}\sum_{i=1}^{2N_0+1} w^{c}_{[i]}(x_j)\phi_{[i]} + \frac{\gamma}{(1-x_j)^{-\beta}(1+x_j)^{-\alpha}}\sum_{m=1}^{3} B_m\phi_{[I+m]} = \frac{P_j}{2\mu_0\mathrm{i}} + \frac{1}{2\mu_0}(q(x_j) - \mathrm{i}p_a(x_j)) \quad j = 1,\ldots,2N_0 \tag{63}$$

$$\sum_{i=1}^{2N_0+1} v_{[i]}(x_j)\phi_{[i]} = 0 \tag{64}$$

in which singular weight functions, $v^c_{[i]}$ and $w^c_{[i]}$, and the Lagrange coefficients, B_m, and parameter I can be found in Kabir et al. (1998).

The discrete forms of Cauchy-type singular integral equation, Eq. (63) and single valuedness condition, Eq. (64) are cast into the matrix form as

$$A^c_{ji}\phi^c_i - B^c_{ji}P_i = g_i \quad i,j = 1,\ldots,N \tag{65}$$

where N is equal to $2N_0 + 1$ and unknown vectors are in the form of

$$\boldsymbol{\phi}^{\mathrm{T}} = \{\phi_{[1]},\ldots,\phi_{t[2N_0+1]}\} \tag{66a}$$

and

$$\mathbf{P}^{\mathrm{T}} = \{P_1,\ldots,P_{2N_0},0\} \tag{66b}$$

This constraint condition arising from the presence of a contact zone is given by

$$\frac{\mathrm{d}}{\mathrm{d}x}V(x_j) = 0 \quad \text{if } P_i = p_r(x_j) \leqslant 0 \tag{67}$$

This condition is applied in an average sense along the contact zone as

$$\int_{t_j}^{t_{j+1}} \vartheta(x)\,\mathrm{d}x = 0 \tag{68}$$

whose discrete form can be written as

$$\mathrm{Re}\{v_{[j]}(x_j)\phi_{[j]} + v_{[j+1]}(x_j)\phi_{[j+1]}\} = 0 \tag{69}$$

Since neither the normal reactions over the contact zone and the extent of the contact zone are not known a priori, Eqs. (58) and (65) are solved through an iterative scheme. The solution procedure starts with the determination of the initial estimate for the extent of contact zone by solving Eq. (58) in the absence of unknown normal tractions. With the initial estimate of the contact zone, Eq. (65) is then solved for the compressive reactions over the contact zone. However, the reactions computed by solving Eq. (65) have an oscillatory behavior. This behavior is corrected by smoothing the reactions along the predicted contact zone. The smoothing of reactions is performed by calculating the reactions at integration points and projecting back onto the collocation points by using linear approximation given in Fig. 5. With the smoothed normal reactions over the contact zone, Eq. (58) is the resolved for the contact zone. This procedure is repeated by continuously updating the extent of the contact zone according to Eq. (67) until convergence is achieved.

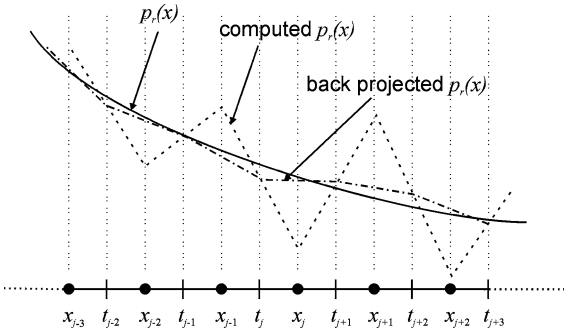

Fig. 5. Schematic for removing numerical noise from computed reactions.

5. Numerical results

The numerical results concern both the uniform pressure and uniform shear loading on the crack surfaces. Poisson's ratios for the materials are specified as $\nu_1 = 0.35$ and $\nu_2 = 0.3$, and the ratio of their shear moduli is specified as $\mu_2/\mu_1 = 20$. The validity of the present analysis results is established by comparison against the finite element predictions.

5.1. Uniform pressure

In the solution of the integral equations for uniform pressure loading, the number of subintervals associated with each unknown functions is chosen as 300 and 500 for the cohesive and interface crack configurations, respectively. In the case of the cohesive crack, the crack opening displacements are symmetric and the sliding displacements are anti-symmetric with respect to the y-axis as expected because of the presence of symmetry in geometry. As shown in Figs. 6 and 7, the present analysis predictions are in remarkable agreement with the finite element results for $h/a = 0.5$. As presented in Table 1, the stress intensity factor for the opening mode decreases as the crack approaches the interface from soft material side. However, the stress intensity factor for the opening mode increases if the crack is approaching the interface from the stiff material side as presented in Table 2. The stress intensity factor associated with the sliding mode increases as the crack approaches the interface either the soft or stiff material side.

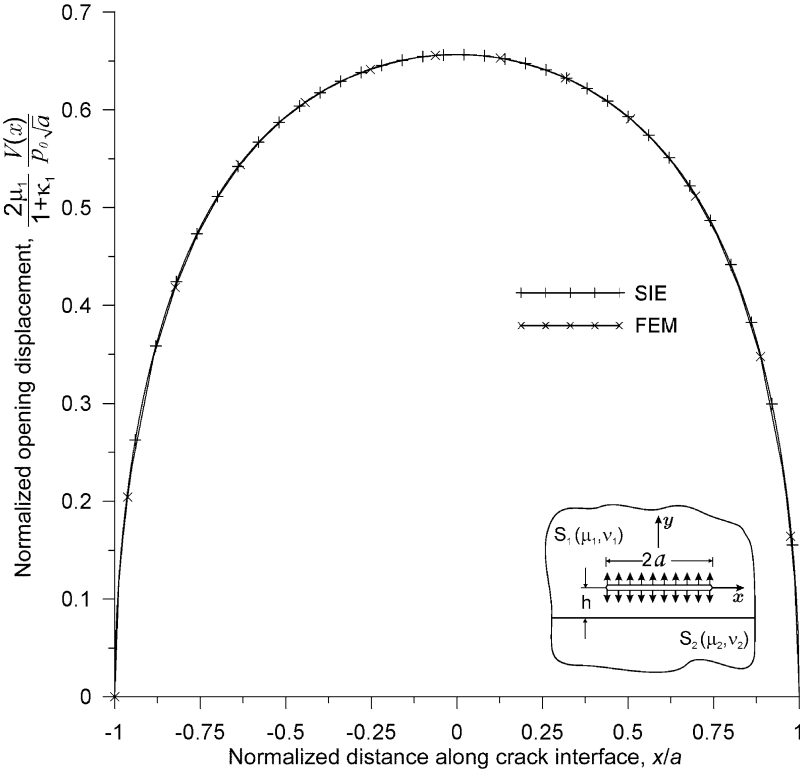

Fig. 6. Opening displacement for a cohesive crack for $h/a = 0.5$.

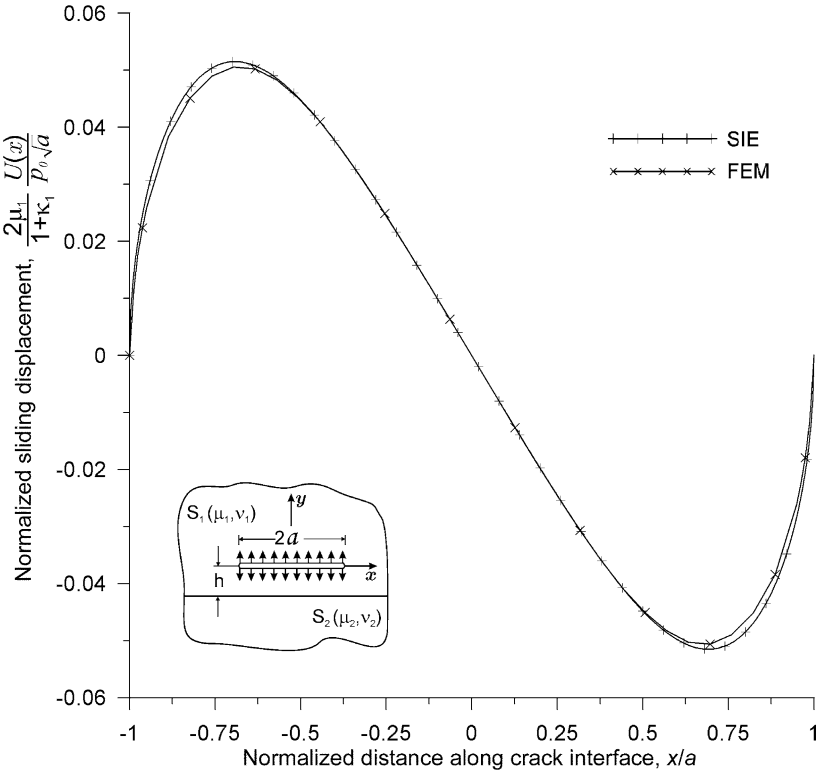

Fig. 7. Sliding displacement for a cohesive crack for $h/a = 0.5$.

Table 1
Normalized stress intensity factors and energy release rates for a pressurized crack ($\mu_2/\mu_1 = 20$, $\nu_1 = 0.35$, $\nu_2 = 0.3$, $p(x) = -p_0$, $q(x) = 0$)

h/a	$\frac{1+\kappa_1}{2\mu_1 p_0}k_1(1)$	$\frac{1+\kappa_1}{2\mu_1 p_0}k_2(1)$	$\frac{4\mu_1}{(1+\kappa_1)p_0^2}\mathscr{G}(1)$
0.2	0.7424	0.1272	0.5674
0.3	0.7583	0.1118	0.5874
0.4	0.7718	0.1010	0.6059
0.5	0.7841	0.0923	0.6233
0.6	0.7955	0.0846	0.6400
0.7	0.8064	0.0773	0.6563
0.8	0.8171	0.0704	0.6725
0.9	0.8275	0.0637	0.6888
1.0	0.8377	0.0573	0.7051
1.5	0.8840	0.0325	0.7825
2.0	0.9178	0.0185	0.8427
2.5	0.9404	0.0111	0.8845
3.0	0.9555	0.0071	0.9130

In the case of an interface crack, the opening displacement is also symmetric and the sliding displacement is anti-symmetric with respect to y-axis as shown in Figs. 8 and 9. As shown in Fig. 10 in which regions S_1

Table 2
Normalized stress intensity factors and energy release rates for a pressurized crack ($\mu_2/\mu_1 = 1/20$, $v_1 = 0.3$, $v_2 = 0.35$, $p(x) = -p_0$, $q(x) = 0$)

h/a	$\frac{1+\kappa_1}{2\mu_1 p_0} k_1(1)$	$\frac{1+\kappa_1}{2\mu_1 p_0} k_2(1)$	$\frac{4\mu_1}{(1+\kappa_1)p_0^2} \mathcal{G}(1)$
0.2	2.5446	0.8383	7.1778
0.3	2.3413	0.7055	5.9793
0.4	2.1215	0.5626	4.8174
0.5	1.9287	0.4415	3.9150
0.6	1.7732	0.3476	3.2651
0.7	1.6504	0.2764	2.8001
0.8	1.5531	0.2224	2.4616
0.9	1.4753	0.1809	2.2093
1.0	1.4123	0.1487	2.0168
1.5	1.2255	0.0632	1.5059
2.0	1.1398	0.0315	1.3002
2.5	1.0943	0.0176	1.1978
3.0	1.0675	0.0107	1.1397

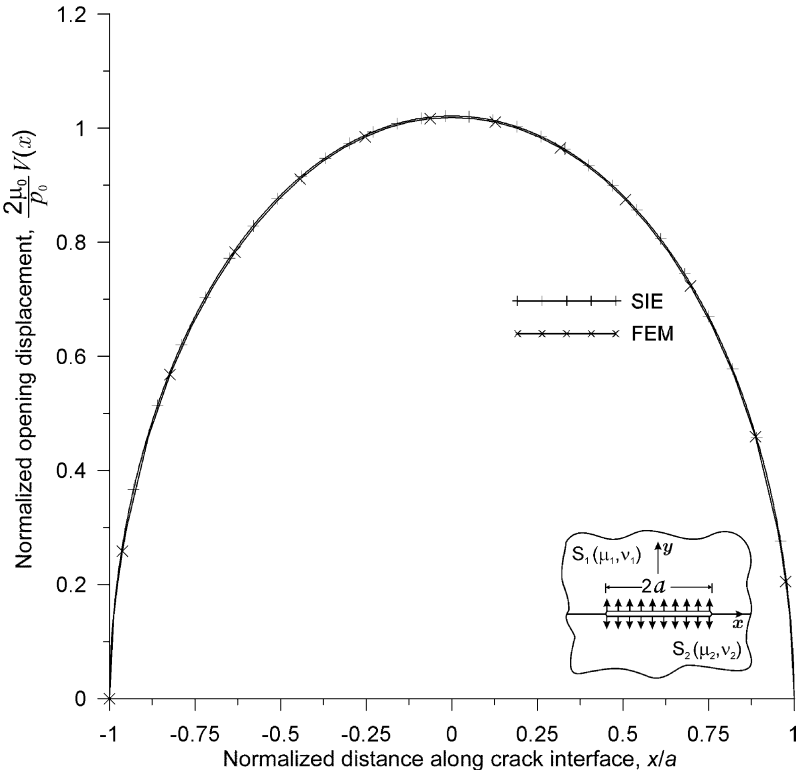

Fig. 8. Opening displacement for an interface crack.

and S_2 represents soft and stiff material sides, respectively, the energy release rate decreases as the crack approaches the interface from the soft material side and it increases if the crack is in the stiff material side.

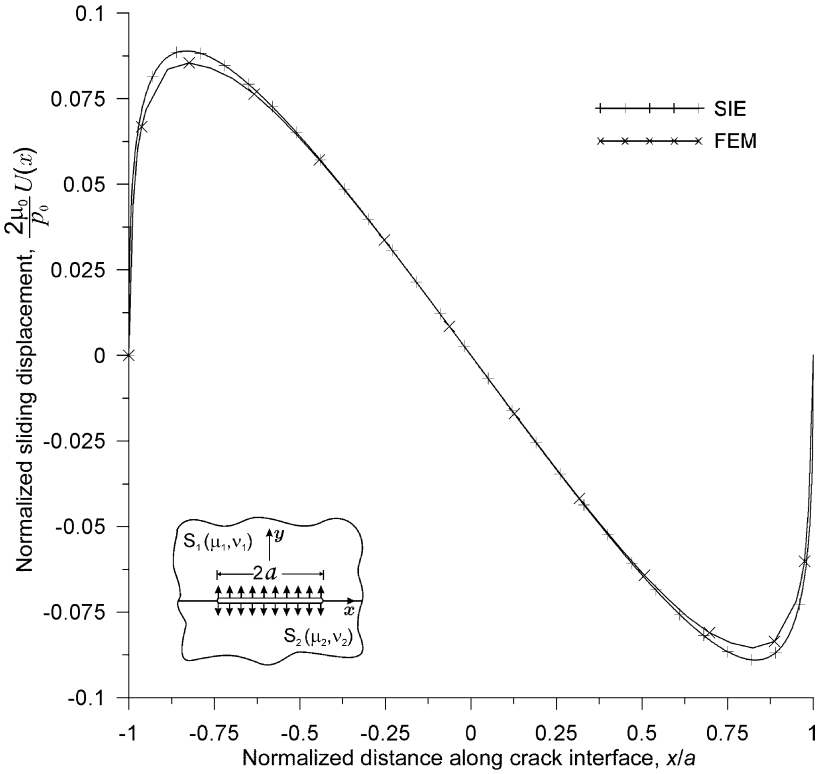

Fig. 9. Sliding displacement for an interface crack.

However, the energy release rate for a crack approaching the interface from the soft material side or stiff material side is asymptotically approaching the value associated with that of the interface crack. Based on the energy release rate criterion, the crack in the soft material away from the interface reaches the critical energy release rate value before the crack close to the interface under the same loading conditions. Thus, the crack away from the interface is more critical than the crack close to the interface if the crack is in the soft material. Based on a similar observation, the crack close to the interface is more critical than the crack away from the interface if the crack is in stiff material.

5.2. Uniform shear

In the solution of the integral equations for uniform shear loading, the number of subintervals associated with each unknown function is chosen as 500 and 1000 for the cohesive and the interface crack configurations, respectively. Although the applied loading is anti-symmetric with respect to the y-axis, results do not exhibit any symmetry because of the existence of the contact zone as shown in Figs. 11–14.

In the case of a cohesive crack, the contact zone and the crack opening displacements are predicted without any numerical oscillations, and compare well with the finite element predictions as shown in Figs. 11 and 12. However, the oscillatory behavior of the singular integral equation associated with the interface crack leads to an oscillatory crack opening and sliding behavior as shown in Figs. 13 and 14. Although these results do not appear to be exactly satisfied, their general (smoothed) behavior also compares well

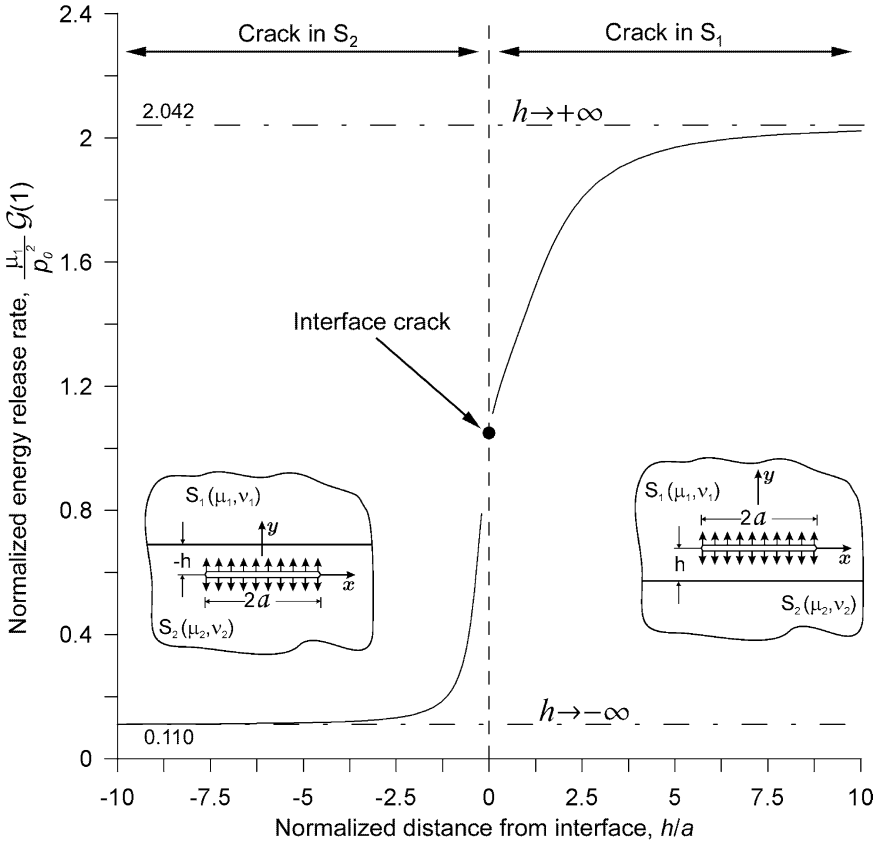

Fig. 10. Variation of energy release rate for a crack under uniform pressure.

with those of the finite element predictions. Furthermore, the length of the contact zone is also in remarkable agreement with the finite element analysis predictions as shown in Fig. 16.

As a result of the contact zone, the stress intensity factors do not have the same magnitudes at the crack tips. Because of the contact zone, the opening mode stress intensity factor is equal to zero at the crack tip where the contact zone occurs. The sliding mode stress intensity factor at contact side of the crack tip is slightly larger than the one at crack tip where no contact zone exists as presented in Tables 3 and 4. However, the energy release rates are similar at both ends of the crack as shown in Fig. 15. The energy release rate for a crack approaching the interface from the soft material side or stiff material side is asymptotically approaching the value associated with that of the interface crack as shown in Fig. 15. Similar to the crack under uniform pressure loading, the crack away from the interface is more critical than the crack close to the interface if the crack is in the soft material. On the contrary, the crack close to the interface is more critical than the crack away from the interface if the crack is in the stiff material side.

As shown in Fig. 16, the length of the contact zones obtained from the singular integral equations and finite element analysis are in remarkable agreement. However, the cracks approaching the interface from the soft material side and the stiff material side do not lead to a common value representative of an interface crack. As the crack approaches to the interface from the stiff material side, the interface behaves like a

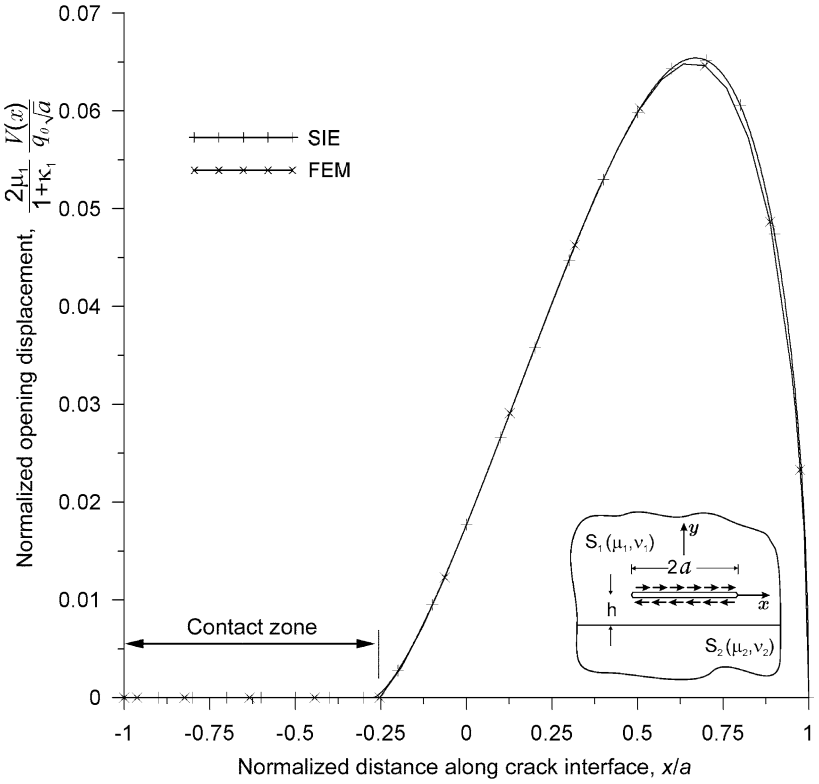

Fig. 11. Opening displacement for a cohesive crack under uniform shear loading for $h/a = 0.5$.

traction-free boundary. Therefore, the contact zone length diminishes because the resistance to crack opening decreases as the crack approaches the interface. On the other hand, when the crack approaches to the interface form the soft material side, the interface behaves like a rigid boundary which leads to an increase in the contact zone length.

6. Conclusions

This study examines the behavior of the energy release rate as the cohesive crack located parallel to the interface approaches the interface from either the soft or the stiff side of the interface while ensuring no interpenetration. The limiting value of the energy release rate is established by considering an interface crack. In order to impose the appropriate constraint conditions on the crack opening displacements, the solution method treats both the crack opening and sliding displacements as primary unknowns. The crack opening displacements are physically more meaningful and readily validated against the finite element analysis predictions. As the cohesive crack approaches the interface from either side of the interface, the energy release rate approaches to that of the interface crack. This is indicative of a continuous behavior for the energy release rate, and that the interface crack is a natural limit of a cohesive crack. However, the length of contact zone on the crack surfaces under uniform shear loading does not approach to that of the interface crack. The results of the present analysis are in remarkable agreement with the finite element predictions.

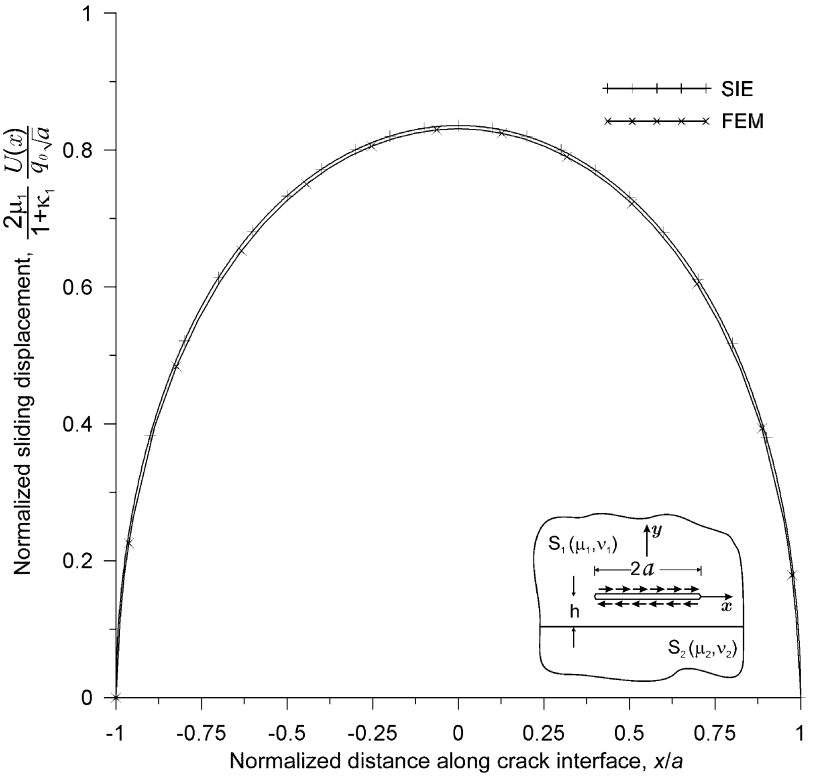

Fig. 12. Sliding displacement for a cohesive crack under uniform shear loading for $h/a = 0.5$.

Appendix A

The explicit form of the coefficients in Eq. (11) are given by

$$A_{11} = (\kappa_1 - 2\alpha h)a_1 e^{-2\alpha h}A_{13} + \frac{\kappa_2\mu_1((1+4\alpha^2h^2-\kappa_1^2)\mu_1 + (\kappa_1^2+\kappa_1-4\alpha^2h^2)\mu_2) - \mu_2(\kappa_1(1+\kappa_1)\mu_1 + 4\alpha^2h^2(\mu_2-\mu_1))}{2\alpha(\mu_2+\kappa_2\mu_1)(\mu_1+\kappa_1\mu_2)} e^{-2\alpha h}A_{14}$$

$$A_{12} = -2\alpha a_1 e^{-2\alpha h}A_{13} + (\kappa_1 + 2\alpha h)a_1 e^{-2\alpha h}A_{14}$$

$$A_{23} = \frac{(1+\kappa_1)\mu_1}{\mu_1+\kappa_1\mu_2}A_{13} + \frac{(1+\kappa_1)\mu_1(-\kappa_1\mu_2 - 2\alpha h((\kappa_2-1)\mu_1 + \mu_2(1-\kappa_1)) + \kappa_2(\mu_1(1-\kappa_1)+\kappa_1\mu_2))}{2\alpha(\mu_2+\kappa_2\mu_1)(\mu_1+\kappa_1\mu_2)}A_{14}$$

$$A_{24} = \frac{(1+\kappa_1)\mu_1}{\kappa_2\mu_1+\mu_2}A_{14}$$

$$A_{31} = [-\kappa_1 + (\kappa_1 - 2\alpha h)a_1 e^{-2\alpha h}]A_{13} + \left\{\frac{\mu_2(4\alpha^2h^2(\mu_1-\mu_2) - \kappa_1(1+\kappa_1)\mu_1) + \kappa_2\mu_1(\mu_1(1-\kappa_1^2+4\alpha^2h^2) + \mu_2(\kappa_1(1+\kappa_1) - 4\alpha^2h^2))}{2\alpha(\mu_2+\kappa_2\mu_1)(\mu_1+\kappa_1\mu_2)} e^{-2\alpha h} + \frac{(\kappa_1^2-1)}{2\alpha}\right\}A_{14}$$

$$A_{32} = (2 - 2a_1 e^{-2\alpha h})\alpha A_{13} - (\kappa_1 - (2\alpha h + \kappa_1)a_1 e^{-2\alpha h})A_{14}$$

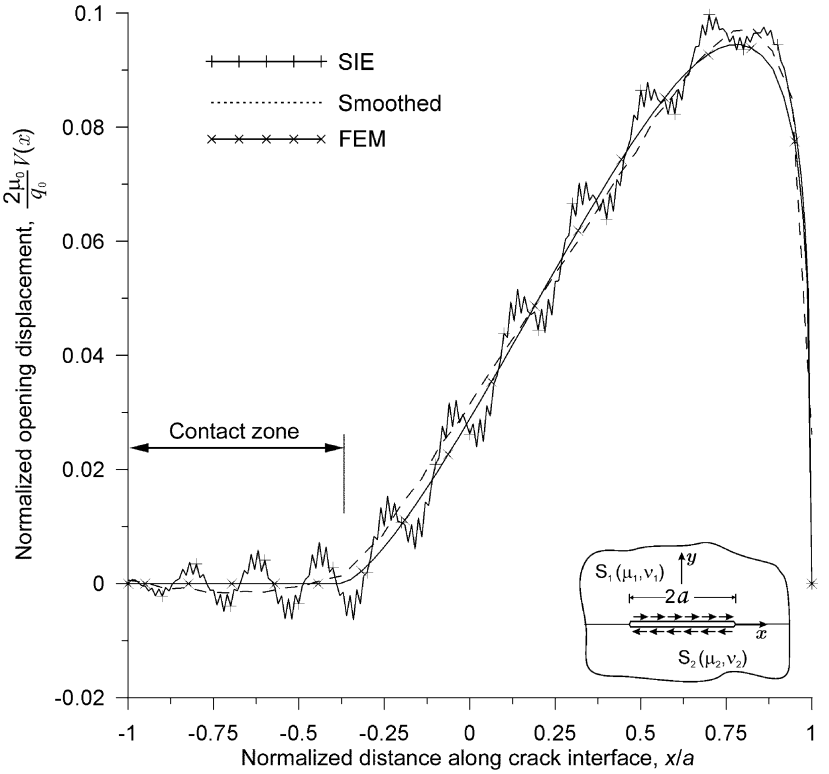

Fig. 13. Opening displacement for an interface crack under uniform shear loading.

The parameters, D_m, h_j and L in Eq. (54) are dependent on the degree of approximation dictated by the value of M which is chosen to be 5 for higher order approximation. Regardless of the order of approximation, the discretization results in a uniform length for each subinterval, and the spacing between the integration points can be expressed as

$$h_j = t_j + 1 - t_j$$

The parameters, L and D_m are defined by using Lagrange's differentiation formulas given by Abramowitz and Stegun (1965), and their explicit form for $M = 5$ is expressed as

$$L = \begin{cases} 0 & j = 1 \\ j-2 & j < N_0 \text{ and } j \neq 1 \\ j-3 & j \geqslant N_0 \text{ and } j \neq 2N_0 \\ 2N_0 - 4 & j = 2N_0 \end{cases}$$

$$D_1(h) = \begin{cases} -11/(12h) & j = 1 \\ -1/(24h) & j < N_0 \text{ and } j \neq 1 \\ 0 & j \geqslant N_0 \text{ and } j \neq 2N_0 \\ -1/(24h) & j = 2N_0 \end{cases}$$

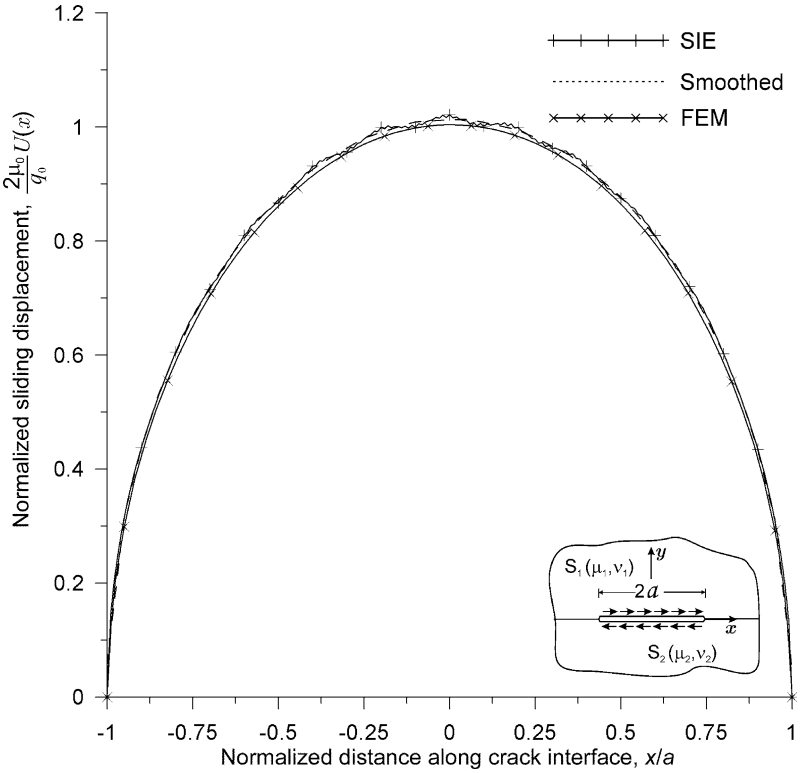

Fig. 14. Sliding displacement for an interface crack under uniform shear loading.

Table 3
Normalized stress intensity factors and energy release rates for a crack under uniform shear ($\mu_2/\mu_1 = 20$, $\nu_1 = 0.35$, $\nu_2 = 0.3$, $p(x) = 0$, $q(x) = -q_0$)

h/a	$\frac{1+\kappa_1}{2\mu_1 q_0}k_1(1)$	$\frac{1+\kappa_1}{2\mu_1 q_0}k_2(1)$	$\frac{1+\kappa_1}{2\mu_1 q_0}k_1(-1)$	$\frac{1+\kappa_1}{2\mu_1 q_0}k_2(-1)$	$\frac{4\mu_1}{(1+\kappa_1)q_0^2}\mathcal{G}(1)$	$\frac{4\mu_1}{(1+\kappa_1)q_0^2}\mathcal{G}(-1)$
0.2	0.1475	0.8028	0.0000	0.8163	0.6662	0.6662
0.3	0.1339	0.8368	0.0000	0.8474	0.7181	0.7181
0.4	0.1236	0.8627	0.0000	0.8715	0.7596	0.7596
0.5	0.1142	0.8823	0.0000	0.8897	0.7915	0.7915
0.6	0.1049	0.8970	0.0000	0.9031	0.8157	0.8157
0.7	0.0957	0.9082	0.0000	0.9133	0.8341	0.8341
0.8	0.0865	0.9171	0.0000	0.9211	0.8485	0.8485
0.9	0.0776	0.9243	0.0000	0.9275	0.8603	0.8603
1.0	0.0692	0.9304	0.0000	0.9329	0.8704	0.8704
1.5	0.0377	0.9525	0.0000	0.9532	0.9087	0.9087
2.0	0.0211	0.9667	0.0000	0.9669	0.9349	0.9349
2.5	0.0125	0.9759	0.0000	0.9760	0.9526	0.9526
3.0	0.0079	0.9820	0.0000	0.9821	0.9644	0.9644

Table 4
Normalized stress intensity factors and energy release rates for a crack under uniform shear ($\mu_2/\mu_1 = 120$, $\nu_1 = 0.3$, $\nu_2 = 0.35$, $p(x) = 0$, $q(x) = -q_0$)

h/a	$\frac{1+\kappa_1}{2\mu_1 q_0}k_1(1)$	$\frac{1+\kappa_1}{2\mu_1 q_0}k_2(1)$	$\frac{1+\kappa_1}{2\mu_1 q_0}k_1(-1)$	$\frac{1+\kappa_1}{2\mu_1 q_0}k_2(-1)$	$\frac{4\mu_1}{(1+\kappa_1)q_0^2}\mathcal{G}(1)$	$\frac{4\mu_1}{(1+\kappa_1)q_0^2}\mathcal{G}(-1)$
0.2	0.0000	1.2843	0.4259	1.2117	1.6494	1.6495
0.3	0.0000	1.1971	0.3789	1.1356	1.4330	1.4330
0.4	0.0000	1.1537	0.3333	1.1045	1.3309	1.3310
0.5	0.0000	1.1289	0.2887	1.0914	1.2744	1.2744
0.6	0.0000	1.1130	0.2476	1.0852	1.2389	1.2389
0.7	0.0000	1.1018	0.2112	1.0813	1.2139	1.2139
0.8	0.0000	1.0930	0.1799	1.0781	1.1946	1.1946
0.9	0.0000	1.0856	0.1532	1.0747	1.1786	1.1786
1.0	0.0000	1.0792	0.1307	1.0712	1.1646	1.1646
1.5	0.0000	1.0545	0.0618	1.0527	1.1120	1.1120
2.0	0.0000	1.0382	0.0323	1.0377	1.0778	1.0778
2.5	0.0000	1.0275	0.0184	1.0274	1.0558	1.0558
3.0	0.0000	1.0205	0.0113	1.0204	1.0414	1.0414

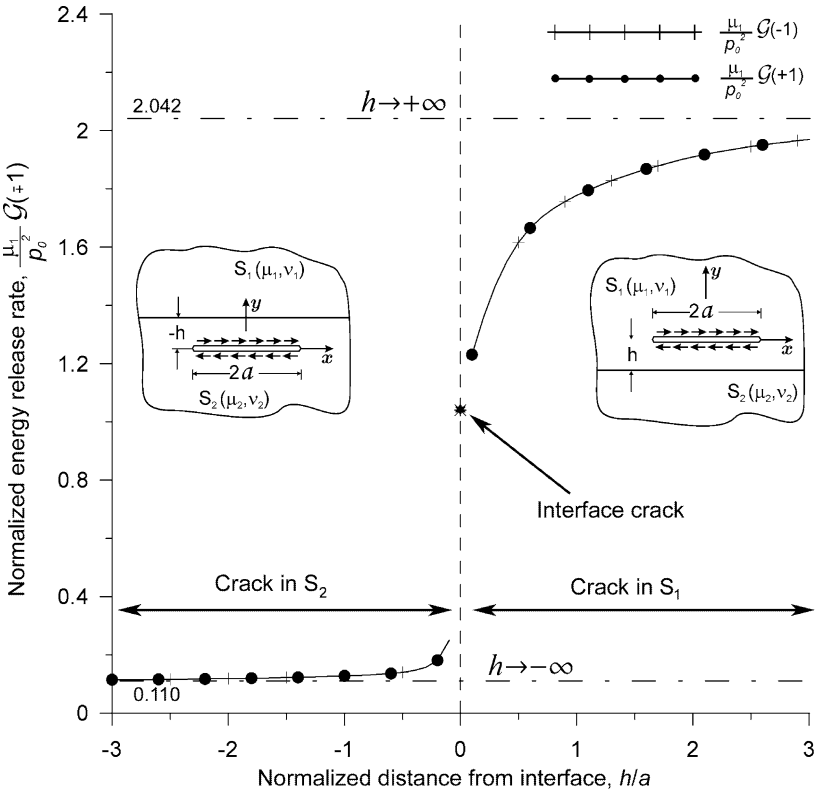

Fig. 15. Variation of energy release rate for a crack under uniform shear.

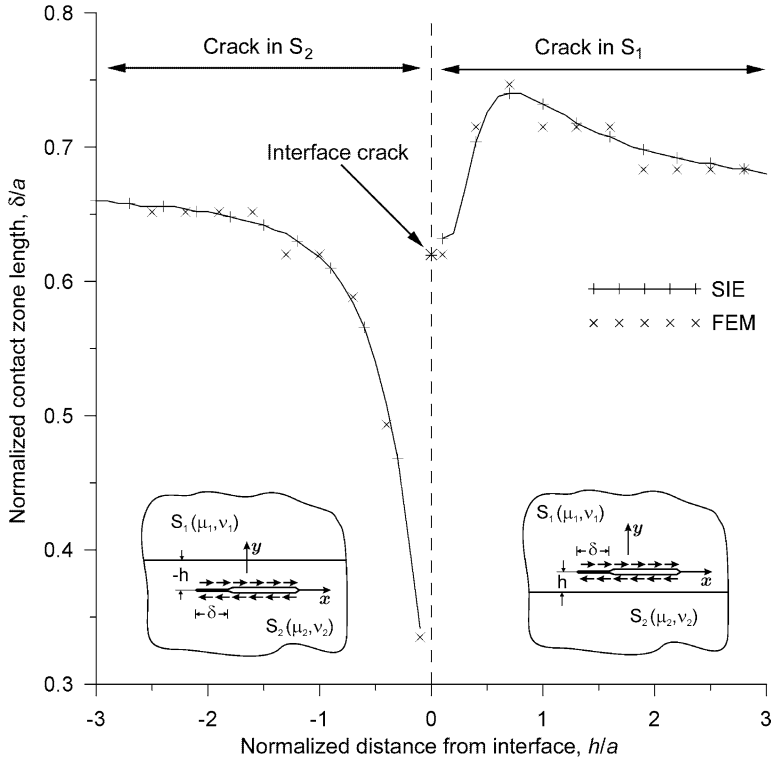

Fig. 16. Length of the contact zone under constant shear loading.

$$D_2(h)=\begin{cases}17/(24h) & j=1\\ -9/(8h) & j<N_0 \text{ and } j\neq 1\\ 1/(24h) & j\geqslant N_0 \text{ and } j\neq 2N_0\\ 5/(24h) & j=2N_0\end{cases}$$

$$D_3(h)=\begin{cases}3/(8h) & j=1\\ 9/(8h) & j<N_0 \text{ and } j\neq 1\\ -9/(8h) & j\geqslant N_0 \text{ and } j\neq 2N_0\\ -3/(8h) & j=2N_0\end{cases}$$

$$D_4(h)=\begin{cases}-5/(24h) & j=1\\ -1/(24h) & j<N_0 \text{ and } j\neq 1\\ 9/(8h) & j\geqslant N_0 \text{ and } j\neq 2N_0\\ -17/(24h) & j=2N_0\end{cases}$$

$$D_5(h)=\begin{cases}1/(24h) & j=1\\ 0 & j<N_0 \text{ and } j\neq 1\\ -1/(24h) & j\geqslant N_0 \text{ and } j\neq 2N_0\\ 11/(12h) & j=2N_0\end{cases}$$

References

Abramowitz, M., Stegun, I.A., 1965. Handbook of Mathematical Functions. Dover Publications, New York.

Atkinson, C., 1977. On stress singularities and interfaces in linear elastic fracture mechanics. International Journal of Fracture 13, 807–820.

Atkinson, C., 1982. The interface crack with a contact zone (An analytical treatment). International Journal of Fracture 18, 161–177.

Chan, Y.-S., Fannjiang, A.C., Paulino, G.H., 2003. Integral equations with hypersingular kernels—theory and applications to fracture mechanics. International Journal of Engineering Science 41, 683–720.

Comninou, M., 1977. The interface crack. Journal of Applied Mechanics 44, 631–636.

Comninou, M., Schmueser, D., 1979. The interface crack in a combined tension–compression and shear field. Journal of Applied Mechanics 46, 345–348.

England, A.H., 1965. A crack between dissimilar media. ASME Journal of Applied Mechanics 32, 400–402.

Erdogan, F., 1965. Stress distribution in bonded dissimilar materials with cracks. ASME – Transactions – Journal of Applied Mechanics 32, 403–410.

Erdogan, F., 1969. Approximate solutions of system of singular integral equations. SIAM Journal of Applied Mathematics 17, 1041–1059.

Erdogan, F., 1971. Bonded dissimilar materials containing cracks parallel to the interface. Engineering Fracture Mechanics 3, 231–240.

Erdogan, F., 1997. Fracture mechanics of interfaces. In: Rossmanith, H.-P. (Ed.), Proceedings of the First International Conference on Damage and Failure of Interfaces. A.A. Balkema, Rotterdom, The Netherlands.

Erdogan, F., Gupta, G.D., 1971a. The stress analysis of multi-layered composites with a flaw. International Journal of Solids and Structures 7, 39–61.

Erdogan, F., Gupta, G.D., 1971b. Layered composites with an interface flaw. International Journal of Solids and Structures 7, 1089–1107.

Erdogan, F., Gupta, G.D., 1972. On the numerical solution of singular integral equations. Quarterly of Applied Mathematics 30, 525–534.

Erdogan, F., Joseph, P.F., 1988. On the mechanics of interfacial zones in bonded materials. Recent Advances in Engineering Science: a symposium dedicated to A. Cemal Eringen, Berkeley, CA, pp. 108–120.

Erdogan, F., Wu, B., 1993. Interface crack problems in layered orthotropic materials. Journal of the Mechanics and Physics of Solids 41, 889–917.

Hutchinson, J.W., Suo, Z., 1992. Mixed mode cracking in layered materials. In: Hutchinson, J.W., Wu, T.Y. (Eds.), Advances in Applied Mechanics, vol. 29. Academic Press, San Diego, pp. 63–191.

Ioakimidis, N.I., 1988a. Mangler-type principal value integrals in hypersingular integral equations for crack problems in plane elasticity. Engineering Fracture Mechanics 31, 895–898.

Ioakimidis, N.I., 1988b. The hypersingular integrodifferential equation of a straight crack along the interface of two bonded isotropic elastic half-planes. International Journal of Fracture 38, R75–R79.

Ioakimidis, N.I., 1990. Generalized Mangler-type principal value integrals in with an application to fracture mechanics. Journal of Computational and Applied Mathematics 30, 227–234.

Irwin, G.R., 1957. Analysis of stresses and strains near the end of a crack traversing a plate. Journal of Applied Mechanics 24, 361–364.

Kabir, H., Madenci, E., Ortega, A., 1998. Numerical solution of integral equations with logarithmic-, Cauchy- and Hadamard-type singularities. International Journal for Numerical Methods in Engineering 41, 617–638.

Kaya, A.C., 1984. Application of integral equations with strong singularities in fracture mechanics. Ph.D. Thesis, Lehigh University, Bethlehem, PA.

Kaya, A.C., Erdogan, F., 1987. On the solution of integral equations with strongly singular kernels. Quarterly of Applied Mathematics 43, 105–122.

Malyshev, B.M., Salganik, R.L., 1965. Strength of adhesive joints using theory of cracks. International Journal of Fracture Mechanics 1, 114–128.

Miller, G.R., Keer, L.M., 1985. A numerical technique for the solution of singular integral equations of the second kind. Quarterly of Applied Mathematics 5, 455–465.

Mulville, D.R., Mast, P.W., Vaisnav, R.N., 1976. Strain energy release rate for interfacial cracks between dissimilar media. Engineering Fracture Mechanics 8, 555–565.

Muskhelishvili, N.I., 1992. Singular Integral Equations, second ed. Dover Publications, New York.

Quan, M.A., 1991. Analysis of a finite interface crack emanating from the junction of three sectors. Ph.D. Thesis, University of California – Los Angeles, Los Angeles, CA.

Rice, J.R., 1988. Elastic fracture mechanics concepts for interfacial cracks. Journal of Applied Mechanics, Transactions ASME 55, 98–103.

Rice, J.R., Sih, G.C., 1965. Plane problems of cracks in dissimilar media. Journal of Applied Mechanics 32, 418–423.

Simonov, I.V., 1990. An interface crack in an inhomogeneous stress field. International Journal of Fracture 46, 223–235.
Suo, Z., Hutchinson, J.W., 1990. Interface crack between two elastic layers. International Journal of Fracture 43, 1–18.
Williams, M.L., 1959. The stresses around a fault or crack in dissimilar media. Bulletin of Seismological Society of America 49, 199–204.